

Chapter 11

Arbitrarily High-Order Time-Stepping Schemes for Nonlinear Klein–Gordon Equations



This chapter presents arbitrarily high-order time-stepping schemes for solving high-dimensional nonlinear Klein–Gordon equations with different boundary conditions. We first formulate an abstract ordinary differential equation (ODE) on a suitable infinite-dimensional function space based on the operator spectrum theory. We then introduce an operator-variation-of-constants formula for the nonlinear abstract ODE. The nonlinear stability and convergence are rigorously analysed once the spatial differential operator is approximated by an appropriate positive semi-definite matrix. With regard to the two dimensional Dirichlet or Neumann boundary problems, the time-stepping schemes coupled with *discrete Fast Sine/Cosine Transformation* can be applied to simulate the two-dimensional nonlinear Klein–Gordon equations effectively. The numerical results demonstrate the advantage of the schemes in comparison with the existing numerical methods for solving nonlinear Klein–Gordon equations in the literature.

11.1 Introduction

The computation of the Klein–Gordon equation which has a nonlinear potential function, is of great importance in a wide range of application areas in science and engineering. The nonlinear potential gives rise to major challenges. In this chapter, we begin with the following nonlinear Klein–Gordon equation in a single space variable:

$$\begin{cases} u_{tt} - a^2 \Delta u = f(u), & t_0 < t \leq T, \quad x \in \Omega, \\ u(x, t_0) = \varphi_1(x), \quad u_t(x, t_0) = \varphi_2(x), & x \in \bar{\Omega}, \end{cases} \quad (11.1)$$

and suppose that the initial valued problem (11.1) is supplemented with the following periodic boundary condition on the domain $\Omega = (-\pi, \pi)$

$$u(x, t) = u(x + 2\pi, t), \quad (11.2)$$

where $u(x, t)$ represents the wave displacement at position x and time t , $\Delta = \frac{\partial^2}{\partial x^2}$, and $f(u)$ is a nonlinear function of u chosen as the negative derivative of a potential energy $V(u) \geq 0$. Generally, there are various choices of the potential function $f(u)$ to investigate solitons and nonlinear phenomena. For instance, the following sine–Gordon equation

$$u_{tt} - a^2 \Delta u + \sin(u) = 0, \quad (11.3)$$

is well known, and other nonlinear potential functions also appear in the literature such as $f(u) = \sinh u$ and polynomial $f(u)$. Moreover, if $u(\cdot, t) \in H^1(\Omega)$ and $u_t(\cdot, t) \in L^2(\Omega)$, energy conservation becomes another key feature of the Klein–Gordon equation, i.e.,

$$E(t) \equiv \frac{1}{2} \int_{\Omega} (u_t^2 + a^2 |\nabla u|^2 + 2V(u)) dx = E(t_0). \quad (11.4)$$

This is an essential property in the theory of solitons. Accordingly, it is also significant to test the effectiveness of a numerical method in preserving the corresponding discrete energy.

In a wide variety of application areas in science and engineering, such as nonlinear optics, solid state physics and quantum field theory [10, 23, 53], the nonlinear wave equation plays an important role and has been extensively investigated. In particular, the nonlinear Klein–Gordon equation (11.1) is used to model many different nonlinear phenomena, including the propagation of dislocations in crystals and the behavior of elementary particles and of Josephson junctions (see Chap. 8.2 in [24] for details). Its description and understanding are very important from both the analytical and numerical aspects, and have been investigated by many researchers. On the analytical front, the Cauchy problem was investigated (see, e.g. [7, 13, 26, 36]). If the potential function satisfies $V(u) \geq 0$ for $u \in \mathbb{R}$, the global existence of solutions for the defocusing case, was established in [13], whereas if the energy potential satisfies $V(u) \leq 0$ for $u \in \mathbb{R}$, the focusing case, possible finite time blow-up was shown in [7]. With regard to the numerical methods, there have been proposed and studied a variety of solution procedures for solving the nonlinear Klein–Gordon equation. For instance, the energy-preserving explicit, semi-implicit and symplectic conservative standard finite difference time domain (FDTD) discretisations were proposed and analysed in [1, 9, 25, 38, 44]. As far as the finite-difference method is concerned, on the basis of standard finite-difference approximations, a three-time-level scheme was derived by Strauss and Vázquez in [47]. Jiménez [35] derived conservative finite difference schemes with some analogous discretisations to that used in [47] for the nonlinear term. Other approaches, such as the finite element method and the spectral method, were also studied in [17, 18, 27, 50]. With respect to finite-element techniques, Tourigny [50] proved that the use of product approximations in Galerkin methods subject to Dirichlet boundary conditions does not affect the convergence

rate of the method. Guo et al. [27] developed a conservative Legendre spectral method. Dehghan et al. used radial basis functions, the dual reciprocity boundary integral equation technique, the collocation and finite-difference collocation methods for solving the nonlinear Klein–Gordon equations, or coupled Klein–Gordon equations (see, e.g. [20–22, 37]). Although many numerical methods have been derived and investigated for solving the nonlinear Klein–Gordon equation in the literature, in general, the existing numerical methods have limited accuracy, and little attention was paid to the special structure brought by spatial discretisations. This motivates the main theme of this chapter, which is to consider arbitrarily high-order Lagrange collocation-type time-stepping schemes for efficiently solving nonlinear Klein–Gordon equations.

The plan of this chapter is as follows. In Sect. 11.2, based on the operator spectrum theory, we first formulate the one-dimensional nonlinear Klein–Gordon equation (11.1)–(11.2) as an abstract second-order ordinary differential equation on an infinite-dimensional Hilbert space $L^2(\Omega)$. Then, the operator-variation-of-constants formula for the abstract equation is introduced, which is in fact an integral equation of the solution for the nonlinear Klein–Gordon equation (11.1)–(11.2). In Sect. 11.3, using the derived operator-variation-of-constants formula, we calculate the nonlinear integrals appearing in this formula by Lagrange interpolation. This leads to a class of arbitrarily high-order Lagrange collocation-type time-stepping schemes. Furthermore, an investigation of the local error bounds is made, which arrives at the simplified order conditions in a much simpler form. Section 11.4 is devoted to semidiscretisation. This process enables us to take advantage of the properties of the undiscretised differential operator \mathcal{A} and incorporate the special structure introduced by spatial discretisations with the new integrators. The main theoretical results of this work are presented in Sect. 11.5. We use the strategy of energy analysis to study the nonlinear stability and convergence of the fully discrete scheme. Since these fully discrete schemes are implicit, iterative solutions are required in practical computations. Therefore, we use fixed-point iteration and analyse its convergence in this section. In Sect. 11.6 we apply the Lagrange collocation-type time integrators to the two-dimensional nonlinear Klein–Gordon equations, equipped with homogenous Dirichlet or Neumann boundary conditions. In a similar way to the one-dimensional periodic boundary case, the abstract ordinary differential equations and the operator-variation-of-constants formula are established on the infinite-dimensional Hilbert space $L^2(\Omega)$. In Sect. 11.7, we are concerned with numerical experiments, and the numerical results show the advantage and effectiveness of our new schemes in comparison with the existing numerical methods in the literature. The last section is devoted to brief conclusions and discussions.

In this chapter, all essential features of the methodology are presented in the one-dimensional and two-dimensional cases, although the schemes to be analysed lend themselves with equal ease to higher dimensions.

11.2 Abstract Ordinary Differential Equation

Motivated by recent interest in exponential integrators for semilinear parabolic problems [30–32], and based on the operator spectrum theory (see, e.g. [6]), we will formulate the nonlinear problem (11.1)–(11.2) as an abstract ordinary differential equation on the Hilbert space $L^2(\Omega)$, and introduce an operator-variation-of-constants formula. To this end, some bounded operator-argument functions will be defined and analysed in advance, because these are essential to introducing the operator-variation-of-constants formula.

To begin with, we define the functions

$$\phi_j(x) := \sum_{k=0}^{\infty} \frac{(-1)^k x^k}{(2k+j)!}, \quad j = 0, 1, 2, \dots, \quad \forall x \geq 0. \quad (11.5)$$

It can be observed that $\phi_j(x)$, $j = 0, 1, 2, \dots$ are bounded functions for any $x \geq 0$. For example, we have

$$\phi_0(x) = \cos(\sqrt{x}), \quad \phi_1(x) = \frac{\sin(\sqrt{x})}{\sqrt{x}}, \quad (11.6)$$

with $\phi_1(0) = 1$, and it is obvious that $|\phi_j(x)| \leq 1$ for $j = 0, 1$ and $\forall x \geq 0$. For an abstract formulation of problem (11.1)–(11.2), we define the linear differential operator \mathcal{A} by

$$(\mathcal{A}v)(x) = -a^2 v_{xx}(x). \quad (11.7)$$

It is known that the linear differential operator \mathcal{A} is an unbounded operator and not defined for every $v \in L^2(\Omega)$. In order to model the periodic boundary condition (11.2), we consider \mathcal{A} on the domain:

$$D(\mathcal{A}) := \{v \in H^2(\Omega) : v(x) = v(x + 2\pi)\}. \quad (11.8)$$

Obviously, the defined operator \mathcal{A} is positive semi definite, i.e.,

$$(\mathcal{A}v(x), v(x)) = \int_0^{2\pi} \mathcal{A}v(x) \cdot v(x) dx = a^2 \int_0^{2\pi} v_x^2(x) dx \geq 0, \quad \forall v(x) \in D(\mathcal{A}).$$

Here, (\cdot, \cdot) denotes the inner product of $L^2(\Omega)$ and integration by parts, or Green's formula, has been used. Moreover, we note the important fact that the operator \mathcal{A} has a complete system of orthogonal eigenfunctions $\{e^{ikx} : k \in \mathbb{Z}\}$ in the Hilbert space $L^2(\Omega)$, and the corresponding eigenvalues are given by $a^2 k^2$, $k = 0, \pm 1, \pm 2, \dots$ (see, e.g. [49]). From the isomorphism between $L^2(\Omega)$ and $l^2 = \{x = (x_i)_{i \in \mathbb{Z}} : \sum_{i \in \mathbb{Z}} |x_i|^2 < +\infty\}$, the operator \mathcal{A} induces a corresponding operator on l^2

(see, e.g. [6, 32]). Then, it can be observed that the functions (11.5) imply the operator functions

$$\phi_j(t\mathcal{A}) : L^2(\Omega) \rightarrow L^2(\Omega),$$

for $j = 0, 1, 2, \dots$ and $t \geq t_0$ as follows:

$$\phi_j(t\mathcal{A})v(x) = \sum_{k=-\infty}^{\infty} \hat{v}_k \phi_j(ta^2k^2)e^{ikx}, \quad \text{for } v(x) = \sum_{k=-\infty}^{\infty} \hat{v}_k e^{ikx}. \quad (11.9)$$

We next show that the defined operator functions are bounded. To do this, we need to clarify the norm of the function in $L^2(\Omega)$, which can be characterised in the frequency space by

$$\|v\|^2 = 2\pi \sum_{k=-\infty}^{\infty} |\hat{v}_k|^2. \quad (11.10)$$

The details can be found in [46]. Therefore, we have

$$\|\phi_j(t\mathcal{A})\|_{L^2(\Omega) \leftarrow L^2(\Omega)}^2 = \sup_{\|v\| \neq 0} \frac{\|\phi_j(t\mathcal{A})v\|^2}{\|v\|^2} \leq \sup_{t \geq t_0} |\phi_j(ta^2k^2)| \leq \gamma_j, \quad (11.11)$$

where γ_j are bounds on the functions $|\phi_j(x)|$ for $j = 0, 1, 2, \dots$ and $x \geq 0$. For instance, we may choose $\gamma_0 = \gamma_1 = 1$ and then

$$\|\phi_0(t\mathcal{A})\|_{L^2(\Omega) \leftarrow L^2(\Omega)}^2 \leq 1 \quad \text{and} \quad \|\phi_1(t\mathcal{A})\|_{L^2(\Omega) \leftarrow L^2(\Omega)}^2 \leq 1. \quad (11.12)$$

By defining $u(t)$ as the function that maps x to $u(x, t)$:

$$u(t) = [x \mapsto u(x, t)],$$

we now can formulate the systems (11.1)–(11.2) as the following abstract ordinary differential equation on the Hilbert space $L^2(\Omega)$:

$$\begin{cases} u''(t) + \mathcal{A}u(t) = f(u(t)) \\ u(t_0) = \varphi_1(x), \quad u'(t_0) = \varphi_2(x). \end{cases} \quad (11.13)$$

With this premise, we are now in a position to present an integral formula for the nonlinear Klein–Gordon equation (11.1)–(11.2). The solution of the abstract ordinary differential equations (11.13) can be given by the operator-variation-of-constants formula summarised in the following theorem.

Theorem 11.1 *The solution of (11.13) and its derivative satisfy*

$$\left\{ \begin{array}{l} u(t) = \phi_0((t-t_0)^2 \mathcal{A})u(t_0) + (t-t_0)\phi_1((t-t_0)^2 \mathcal{A})u'(t_0) \\ \quad + \int_{t_0}^t (t-\zeta)\phi_1((t-\zeta)^2 \mathcal{A})f(u(\zeta))d\zeta, \\ u'(t) = -(t-t_0)\mathcal{A}\phi_1((t-t_0)^2 \mathcal{A})u(t_0) + \phi_0((t-t_0)^2 \mathcal{A})u'(t_0) \\ \quad + \int_{t_0}^t \phi_0((t-\zeta)^2 \mathcal{A})f(u(\zeta))d\zeta, \end{array} \right. \quad (11.14)$$

for $t \in [t_0, T]$, where $\phi_0((t-t_0)^2 \mathcal{A})$ and $\phi_1((t-t_0)^2 \mathcal{A})$ are bounded functions of the operator \mathcal{A} .

Proof Applying the Duhamel Principle to Eqs. (11.1) or (11.13), we have

$$\begin{pmatrix} u(t) \\ u'(t) \end{pmatrix} = e^{\mathcal{J}(t-t_0)} \begin{pmatrix} u(t_0) \\ u'(t_0) \end{pmatrix} + \int_{t_0}^t e^{\mathcal{J}(t-\zeta)} \begin{pmatrix} 0 \\ f(u(\zeta)) \end{pmatrix} d\zeta, \quad (11.15)$$

where

$$\mathcal{J} = \begin{pmatrix} 0 & I \\ -\mathcal{A} & 0 \end{pmatrix}.$$

After expanding the exponential operator through its Taylor series, we obtain

$$e^{\mathcal{J}(t-t_0)} = \sum_{k=0}^{+\infty} \frac{\mathcal{J}^k (t-t_0)^k}{k!}.$$

An argument by induction leads to the following results

$$\mathcal{J}^k = (-1)^{[k/2]} \begin{pmatrix} \frac{1+(-1)^k}{2} \mathcal{A}^{[k/2]} & \frac{1-(-1)^k}{2} \mathcal{A}^{[k/2]} \\ -\frac{1-(-1)^k}{2} \mathcal{A}^{[k/2]+1} & \frac{1+(-1)^k}{2} \mathcal{A}^{[k/2]} \end{pmatrix}, \quad \forall k \in \mathbb{N},$$

where $[k/2]$ denotes the integer part of $k/2$. According to the definition of $\phi_j(\mathcal{A})$ and a careful calculation, we obtain

$$e^{\mathcal{J}(t-t_0)} = \begin{pmatrix} \phi_0((t-t_0)^2 \mathcal{A}) & (t-t_0)\phi_1((t-t_0)^2 \mathcal{A}) \\ -(t-t_0)\mathcal{A}\phi_1((t-t_0)^2 \mathcal{A}) & \phi_0((t-t_0)^2 \mathcal{A}) \end{pmatrix}.$$

The conclusion of the theorem can be obtained straightforwardly by inserting the expansion into (11.15). \square

Remark 11.1 Although equation (11.1) is one-dimensional in space, the method of analysis introduced in this section can be extended to the considerably more important high-dimensional Klein–Gordon equations

$$u_{tt} - a^2 \Delta u = f(u), \quad t \geq t_0, \quad \mathbf{x} \in [-\pi, \pi]^d, \quad (11.16)$$

where $u = u(\mathbf{x}, t)$ and $\Delta = \sum_{i=1}^d \frac{\partial^2}{\partial x_i^2}$, with periodic boundary conditions. In latter case, if we define the operator as the form $\mathcal{A} = -a^2\Delta$, the same operator-variation-of-constants formula as (11.14) for (11.16) can be achieved as well. An application of this approach can be found in a recent paper [56].

Remark 11.2 For the nonlinear Klein–Gordon equation, the formula (11.14) is a nonlinear integral equation which reflects the changes of the solution with time t . It will be helpful in deriving and analysing novel numerical integrators for the nonlinear Klein–Gordon equations. However, if the right-hand function f does not depend on u , i.e.,

$$\begin{cases} u_{tt} - a^2\Delta u = f(\mathbf{x}, t), & t_0 < t \leq T, \mathbf{x} \in \Omega, \\ u(\mathbf{x}, t_0) = \varphi_1(\mathbf{x}), u_t(\mathbf{x}, t_0) = \varphi_2(\mathbf{x}), \end{cases} \tag{11.17}$$

this is a linear or homogenous ($f(\mathbf{x}, t) = 0$) wave equation. The closed-form solution to the linear problem (11.17) can be obtained by using the operator-variation-of-constants formula.

As an illustrative example, we consider the following two-dimensional homogenous periodic wave equation

$$\begin{cases} u_{tt} - a^2(u_{xx} + u_{yy}) = 0, & (x, y) \in (0, 2) \times (0, 2), t > 0, \\ u|_{t=0} = \sin(3\pi x) \sin(4\pi y), u_t|_{t=0} = 0. \end{cases} \tag{11.18}$$

The homogenous problem is equipped with periodic boundary conditions

$$u(x + L_x, y, t) = u(x, y + L_y, t) = u(x, y, t) \tag{11.19}$$

with the fundamental periods $L_x = \frac{2}{3}$ and $L_y = \frac{1}{2}$. Applying the formula (11.14) to (11.18) leads to

$$\begin{cases} u(x, y, t) = \phi_0(t^2\mathcal{A}) \sin(3\pi x) \sin(4\pi y), \\ u_t(x, y, t) = t a^2 \Delta \phi_1(t^2\mathcal{A}) \sin(3\pi x) \sin(4\pi y). \end{cases} \tag{11.20}$$

It follows from a simple calculation that

$$\begin{cases} u(x, y, t) = \sin(3\pi x) \sin(4\pi y) \cos(5t), \\ u_t(x, y, t) = -5 \sin(3\pi x) \sin(4\pi y) \sin(5t), \end{cases} \tag{11.21}$$

which is exactly the solution of problem (11.18) and its derivative.

We next consider the following nonhomogeneous linear wave equation

$$\begin{cases} u_{tt} - (u_{xx} + u_{yy}) = \pi^2 \sin(\pi(x - t)) \sin(\pi y), \\ u|_{t=0} = \sin(\pi x) \sin(\pi y), u_t|_{t=0} = -\pi \cos(\pi x) \sin(\pi y), \end{cases} \tag{11.22}$$

and suppose that the problem is subject to the periodic boundary conditions

$$u(x + L, y, t) = u(x, y + L, t) = u(x, y, t), \quad (11.23)$$

with the fundamental periods $L = 2$. Applying formula (11.14) to (11.22) yields

$$\left\{ \begin{array}{l} u(x, y, t) = \phi_0(t^2 \Delta) \sin(\pi x) \sin(\pi y) - \pi t \phi_1(t^2 \Delta) \cos(\pi x) \sin(\pi y) \\ \quad + \pi^2 \int_0^t (t - \zeta) \phi_1((t - \zeta)^2 \Delta) \sin(\pi(x - \zeta)) \sin(\pi y) d\zeta, \\ u_t(x, y, t) = t \Delta \phi_1(t^2 \Delta) \sin(\pi x) \sin(\pi y) - \pi \phi_0(t^2 \Delta) \cos(\pi x) \sin(\pi y) \\ \quad + \pi^2 \int_0^t \phi_0((t - \zeta)^2 \Delta) \sin(\pi(x - \zeta)) \sin(\pi y) d\zeta. \end{array} \right. \quad (11.24)$$

It follows from a careful calculation that

$$\begin{aligned} \phi_0(t^2 \Delta) \sin(\pi x) \sin(\pi y) &= \sin(\pi x) \sin(\pi y) \cos(\sqrt{2}\pi t), \\ -\pi t \phi_1(t^2 \Delta) \cos(\pi x) \sin(\pi y) &= -\frac{1}{\sqrt{2}} \cos(\pi x) \sin(\pi y) \sin(\sqrt{2}\pi t), \\ \pi^2 \int_0^t (t - \zeta) \phi_1((t - \zeta)^2 \Delta) \sin(\pi(x - \zeta)) \sin(\pi y) d\zeta \\ &= \frac{\pi}{\sqrt{2}} \int_0^t \sin(\sqrt{2}\pi(t - \zeta)) \sin(\pi(x - \zeta)) \sin(\pi y) d\zeta. \end{aligned}$$

We finally obtain the exact solution

$$\begin{aligned} u(x, y, t) &= \sin(\pi x) \sin(\pi y) \cos(\sqrt{2}\pi t) - \frac{1}{\sqrt{2}} \cos(\pi x) \sin(\pi y) \sin(\sqrt{2}\pi t) \\ &\quad + \frac{\pi}{\sqrt{2}} \int_0^t \sin(\sqrt{2}\pi(t - \zeta)) \sin(\pi(x - \zeta)) \sin(\pi y) d\zeta \\ &= \sin(\pi(x - t)) \sin(\pi y), \end{aligned} \quad (11.25)$$

and its derivative

$$u_t(x, y, t) = -\pi \cos(\pi(x - t)) \sin(\pi y). \quad (11.26)$$

11.3 Formulation of the Lagrange Collocation-Type Time Integrators

In light of the useful approach to dealing with the semiclassical Schrödinger equation (see [8]), this analysis will omit the standard steps of first semidiscretising in space and then approximating the semidiscretisation. In this section, based on the for-

mula (11.14), we devote ourselves to constructing arbitrarily high-order Lagrange collocation-type time integrators for the nonlinear system (11.13) in the infinite-dimensional Hilbert space $L^2(\Omega)$. Furthermore, the local error bounds for the constructed time integrators will also be considered in detail.

11.3.1 Construction of the Time Integrators

From Theorem 11.1, the solution of (11.13) and its derivative at time $t_{n+1} = t_n + \Delta t$ for $n = 0, 1, 2, \dots$ are given by

$$\begin{cases} u(t_{n+1}) = \phi_0(\mathcal{V})u(t_n) + \Delta t \phi_1(\mathcal{V})u'(t_n) \\ \quad + \Delta t^2 \int_0^1 (1-z)\phi_1((1-z)^2\mathcal{V})\tilde{f}(t_n + z\Delta t)dz, \\ u'(t_{n+1}) = -\Delta t \mathcal{A} \phi_1(\mathcal{V})u(t_n) + \phi_0(\mathcal{V})u'(t_n) \\ \quad + \Delta t \int_0^1 \phi_0((1-z)^2\mathcal{V})\tilde{f}(t_n + z\Delta t)dz, \end{cases} \quad (11.27)$$

where $\mathcal{V} = \Delta t^2 \mathcal{A}$ and $\tilde{f}(t_n + z\Delta t) = f(u(t_n + z\Delta t))$.

In what follows, we pay our attention to deriving efficient methods for approximating the following two nonlinear integrals:

$$\begin{aligned} I_1 &:= \int_0^1 (1-z)\phi_1((1-z)\mathcal{V})\tilde{f}(t_n + z\Delta t)dz, \\ I_2 &:= \int_0^1 \phi_0((1-z)\mathcal{V})\tilde{f}(t_n + z\Delta t)dz. \end{aligned} \quad (11.28)$$

We choose non-confluent collocation nodes c_1, \dots, c_s and approximate the function $\tilde{f}(t_n + z\Delta t)$ involved in the integrals in (11.28) by its Lagrange interpolation polynomial at these quadrature nodes

$$\begin{aligned} \tilde{f}(t_n + z\Delta t) &= \sum_{i=1}^s l_i(z)\tilde{f}(t_n + c_i\Delta t) + R_s(t_n + z\Delta t) \\ &= \sum_{i=1}^s l_i(z)f(u(t_n + c_i\Delta t)) + R_s(t_n + z\Delta t). \end{aligned} \quad (11.29)$$

Here, $l_i(z)$ for $i = 1, 2, \dots, s$ are the well-known Lagrange basis polynomials

$$l_i(z) = \prod_{\substack{j=1 \\ j \neq i}}^s \frac{z - c_j}{c_i - c_j}, \quad i = 1, 2, \dots, s. \quad (11.30)$$

It is obvious that there exists a constant β satisfies $\max_{1 \leq i \leq s} \max_{0 \leq z \leq 1} |l_i(z)| \leq \beta$. Moreover, the interpolation error on $[0, 1]$ is given by

$$\begin{aligned} R_s(t_n + z\Delta t) &= \tilde{f}(t_n + z\Delta t) - \sum_{i=1}^s l_i(z) \tilde{f}(t_n + c_i \Delta t) \\ &= \frac{\Delta t^s}{s!} \tilde{f}_t^{(s)}(t_n + \xi^n \Delta t) w_s(z), \quad \xi^n \in (0, 1), \end{aligned} \quad (11.31)$$

where $w_s(z) = \prod_{i=1}^s (z - c_i)$ and $\tilde{f}_t^{(j)}(t)$ denotes the j th order derivative of $f(u(t))$ with respect to t .

Suppose that the following approximations have been given:

$$u^n \approx u(t_n), \quad U^{ni} \approx u(t_n + c_i \Delta t).$$

Replacing $\tilde{f}(z)$ in (11.27) by the Lagrange interpolation (11.29) yields approximations to the exact solution and its derivative at time t_{n+1}

$$u^{n+1} = \phi_0(\mathcal{V})u^n + \Delta t \phi_1(\mathcal{V})u^n + \Delta t^2 \sum_{i=1}^s b_i(\mathcal{V})f(U^{ni}), \quad (11.32)$$

$$u^{m+1} = -\Delta t \mathcal{A} \phi_1(\mathcal{V})u^n + \phi_0(\mathcal{V})u^n + \Delta t \sum_{i=1}^s \bar{b}_i(\mathcal{V})f(U^{ni}), \quad (11.33)$$

where $b_i(\mathcal{V})$ and $\bar{b}_i(\mathcal{V})$ are determined by

$$b_i(\mathcal{V}) = \int_0^1 (1-z)\phi_1((1-z)^2\mathcal{V})l_i(z)dz, \quad (11.34)$$

$$\bar{b}_i(\mathcal{V}) = \int_0^1 \phi_0((1-z)^2\mathcal{V})l_i(z)dz. \quad (11.35)$$

It follows from (11.12) that

$$\|b_i(\mathcal{V})\|_{L^2(\Omega) \leftarrow L^2(\Omega)} \leq \max_{0 \leq z \leq 1} |l_i(z)| \leq \beta \quad \text{and} \quad \|\bar{b}_i(\mathcal{V})\|_{L^2(\Omega) \leftarrow L^2(\Omega)} \leq \max_{0 \leq z \leq 1} |l_i(z)| \leq \beta,$$

and this means that $b_i(\mathcal{V})$ and $\bar{b}_i(\mathcal{V})$ are uniformly bounded.

Moreover, we note that the basis $l_i(z)$ for $i = 1, \dots, s$ are polynomials of degree at most $s - 1$, the coefficients $b_i(\mathcal{V})$ are linear combinations of the functions

$$\int_0^1 (1-z)\phi_1((1-z)^2\mathcal{V})z^j dz = \Gamma(j+1)\phi_{j+2}(\mathcal{V}), \quad (11.36)$$

and the coefficients $\bar{b}_i(\mathcal{V})$ are linear combinations of the functions

$$\int_0^1 \phi_0((1-z)^2 \mathcal{V}) z^j dz = \Gamma(j+1) \phi_{j+1}(\mathcal{V}), \tag{11.37}$$

where $\Gamma(j+1)$ is the Gamma function with $\Gamma(1) = 1$ (see, e.g. Abramowitz and Stegun [3]). Recall that, the Gamma function $\Gamma(j+1)$ satisfies the following recursion

$$\Gamma(j+1) = j\Gamma(j) = \dots = j!$$

It remains to determine the approximation U^{ni} . In a similar way to the formula (11.32), we replace Δt by $c_i \Delta t$ to define the internal stages:

$$U^{ni} = \phi_0(c_i^2 \mathcal{V}) u^n + c_i \Delta t \phi_1(c_i^2 \mathcal{V}) u^n + c_i^2 \Delta t^2 \sum_{j=1}^s a_{ij}(\mathcal{V}) f(U^{nj}), \tag{11.38}$$

where it is required that the weights $a_{ij}(\mathcal{V})$ are uniformly bounded. The weights $a_{ij}(\mathcal{V})$ will be determined by suitable order conditions, and we will derive these order conditions in Sect. 11.3.2.

On the basis of the above analysis and the formula (11.27), we present the following Lagrange collocation-type time-stepping integrators for the nonlinear system (11.13).

Definition 11.1 A Lagrange collocation-type time-stepping integrator for solving the nonlinear system (11.13) is defined by

$$\left\{ \begin{aligned} u^{n+1} &= \phi_0(\mathcal{V}) u^n + \Delta t \phi_1(\mathcal{V}) u^n + \Delta t^2 \sum_{i=1}^s b_i(\mathcal{V}) f(U^{ni}), \\ u^{n+1} &= -\Delta t \mathcal{A} \phi_1(\mathcal{V}) u^n + \phi_0(\mathcal{V}) u^n + \Delta t \sum_{i=1}^s \bar{b}_i(\mathcal{V}) f(U^{ni}), \\ U^{ni} &= \phi_0(c_i^2 \mathcal{V}) u^n + c_i \Delta t \phi_1(c_i^2 \mathcal{V}) u^n + c_i^2 \Delta t^2 \sum_{j=1}^s a_{ij}(\mathcal{V}) f(U^{nj}), \quad i = 1, 2, \dots, s, \end{aligned} \right. \tag{11.39}$$

where $b_i(\mathcal{V})$ and $\bar{b}_i(\mathcal{V})$ are defined by (11.34) and (11.35), respectively, and $a_{ij}(\mathcal{V})$ are uniformly bounded.

11.3.2 Error Analysis for the Lagrange Collocation-Type Time-Stepping Integrators

In this subsection, we will analyse the local error bounds of the Lagrange collocation-type time discretisations (11.39) for the nonlinear system (11.13). Our main hypothesis on the nonlinearity f is described below.

Assumption 1 It is assumed that (11.13) possesses a sufficiently smooth solution, and that $f : D(\mathcal{A}) \rightarrow \mathbb{R}$ is sufficiently often Fréchet differentiable in a strip along the exact solution.

Assumption 2 Let f be locally Lipschitz-continuous in a strip along the exact solution $u(t)$. Thus, there exists a real number L such that

$$\|f(v(t)) - f(w(t))\| \leq L\|v(t) - w(t)\| \quad (11.40)$$

for all $t \in [t_0, T]$ and $\max(\|v(t) - u(t)\|, \|w(t) - u(t)\|) \leq R$.

Inserting the exact solution into the time integrators (11.39) yields

$$\begin{cases} u(t_{n+1}) = \phi_0(\mathcal{V})u(t_n) + \Delta t \phi_1(\mathcal{V})u'(t_n) + \Delta t^2 \sum_{i=1}^s b_i(\mathcal{V})\tilde{f}(t_n + c_i \Delta t) + \delta^{n+1}, \\ u'(t_{n+1}) = -\Delta t \mathcal{A} \phi_1(\mathcal{V})u(t_n) + \phi_0(\mathcal{V})u'(t_n) + \Delta t \sum_{i=1}^s \bar{b}_i(\mathcal{V})\tilde{f}(t_n + c_i \Delta t) + \delta^{m+1}, \\ u(t_n + c_i \Delta t) = \phi_0(c_i^2 \mathcal{V})u(t_n) + c_i \Delta t \phi_1(c_i^2 \mathcal{V})u'(t_n) + c_i^2 \Delta t^2 \sum_{j=1}^s a_{ij}(\mathcal{V})\tilde{f}(t_n + c_j \Delta t) + \Delta^{ni}, \\ i = 1, 2, \dots, s, \end{cases} \quad (11.41)$$

where $b_i(\mathcal{V})$ and $\bar{b}_i(\mathcal{V})$ are defined by (11.34) and (11.35), respectively, and $a_{ij}(\mathcal{V})$ are uniformly bounded.

Applying the Lagrange interpolation polynomial (11.29) to the nonlinear integrals in the operator-variation-of-constants formula (11.27), and comparing with the first two equations of (11.41), we obtain the residuals δ^{n+1} and δ^{m+1} :

$$\begin{aligned} \delta^{n+1} &= \frac{\Delta t^{s+2}}{s!} \int_0^1 (1-z)\phi_1((1-z)^2 \mathcal{V})w_s(z)dz f_t^{(s)}(u(t_n + \xi^n \Delta t)), \\ \delta^{m+1} &= \frac{\Delta t^{s+1}}{s!} \int_0^1 \phi_0((1-z)^2 \mathcal{V})w_s(z)dz f_t^{(s)}(u(t_n + \xi^n \Delta t)). \end{aligned} \quad (11.42)$$

It follows from (11.42) that

$$\|\delta^{n+1}\| \leq C_1 \Delta t^{s+2} \quad \text{and} \quad \|\delta^{m+1}\| \leq C_1 \Delta t^{s+1}, \quad (11.43)$$

where

$$C_1 = \frac{1}{s!} \max_{0 \leq z \leq 1} |w_s(z)| \max_{t_0 \leq t \leq T} \|f_t^{(s)}(u(t))\| \quad (11.44)$$

is a constant.

In order to clarify the representation of the residuals Δ^{ni} , we expand $\tilde{f}(t_n + z \Delta t)$ into a Taylor series with remainder in integral form:

$$\tilde{f}(t_n + z\Delta t) = \sum_{k=1}^s \frac{z^{k-1} \Delta t^{k-1}}{(k-1)!} \tilde{f}_t^{(k-1)}(t_n) + \frac{\Delta t^s}{(s-1)!} \int_0^z \tilde{f}_t^{(s)}(t_n + \sigma \Delta t) (z - \sigma)^{s-1} d\sigma. \quad (11.45)$$

On the one hand, inserting the Taylor formula (11.45) into the right-hand side of the operator-variation-of-constants formula gives

$$\begin{aligned} u(t_n + c_i \Delta t) &= \phi_0(c_i^2 \mathcal{V}) u(t_n) + c_i \Delta t \phi_1(c_i^2 \mathcal{V}) u'(t_n) + \sum_{k=1}^s c_i^{k+1} \Delta t^{k+1} \phi_{k+1}(c_i^2 \mathcal{V}) \tilde{f}_t^{(k-1)}(t_n) \\ &\quad + \frac{c_i^{s+2} \Delta t^{s+2}}{(s-1)!} \int_0^1 (1-z) \phi_1((1-z)^2 \mathcal{V}) \int_0^z \tilde{f}_t^{(s)}(t_n + \sigma c_i \Delta t) (z - \sigma)^{s-1} d\sigma dz. \end{aligned} \quad (11.46)$$

Substituting the Taylor formula (11.45) into the right-hand side of the last equations for $i = 1, 2, \dots, s$ of (11.41) yields

$$\begin{aligned} u(t_n + c_i \Delta t) &= \phi_0(c_i^2 \mathcal{V}) u(t_n) + c_i \Delta t \phi_1(c_i^2 \mathcal{V}) u'(t_n) \\ &\quad + \sum_{k=1}^s c_i^2 \Delta t^{k+1} \sum_{j=1}^s a_{ij}(\mathcal{V}) \frac{c_j^{k-1}}{(k-1)!} \tilde{f}_t^{(k-1)}(t_n) \\ &\quad + \frac{c_i^2 \Delta t^{s+2}}{(s-1)!} \sum_{j=1}^s a_{ij}(\mathcal{V}) \int_0^{c_j} \tilde{f}_t^{(s)}(t_n + \sigma \Delta t) (c_j - \sigma)^{s-1} d\sigma + \Delta^{ni}. \end{aligned} \quad (11.47)$$

Subtracting (11.46) from (11.47), we obtain

$$\begin{aligned} \Delta^{ni} &= \sum_{k=1}^s c_i^2 \Delta t^{k+1} \left(c_i^{k-1} \phi_{k+1}(c_i^2 \mathcal{V}) - \sum_{j=1}^s a_{ij}(\mathcal{V}) \frac{c_j^{k-1}}{(k-1)!} \right) \tilde{f}_t^{(k-1)}(t_n) \\ &\quad + \frac{c_i^{s+2} \Delta t^{s+2}}{(s-1)!} \int_0^1 (1-z) \phi_1((1-z)^2 \mathcal{V}) \int_0^z \tilde{f}_t^{(s)}(t_n + \sigma c_i \Delta t) (z - \sigma)^{s-1} d\sigma dz \\ &\quad - \frac{c_i^2 \Delta t^{s+2}}{(s-1)!} \sum_{j=1}^s a_{ij}(\mathcal{V}) \int_0^{c_j} \tilde{f}_t^{(s)}(t_n + \sigma \Delta t) (c_j - \sigma)^{s-1} d\sigma. \end{aligned}$$

By the following order conditions:

$$\sum_{j=1}^s a_{ij}(\mathcal{V}) \frac{c_j^{k-1}}{(k-1)!} = c_i^{k-1} \phi_{k+1}(c_i^2 \mathcal{V}), \quad k = 1, 2, \dots, s, \quad i = 1, 2, \dots, s, \quad (11.48)$$

the residuals Δ^{ni} can be explicitly expressed as:

$$\begin{aligned} \Delta^{ni} &= \frac{c_i^{s+2} \Delta t^{s+2}}{(s-1)!} \int_0^1 (1-z) \phi_1((1-z)^2 \mathcal{V}) \int_0^z \tilde{f}_t^{(s)}(t_n + \sigma c_i \Delta t) (z - \sigma)^{s-1} d\sigma dz \\ &\quad - \frac{c_i^2 \Delta t^{s+2}}{(s-1)!} \sum_{j=1}^s a_{ij}(\mathcal{V}) \int_0^{c_j} \tilde{f}_t^{(s)}(t_n + \sigma \Delta t) (c_j - \sigma)^{s-1} d\sigma. \end{aligned} \quad (11.49)$$

Likewise, we can deduce the following results

$$\|\Delta^{ni}\| \leq \frac{c_i^2 \Delta t^{s+2}}{(s-1)!} \left(c_i^s + \gamma \sum_{i=1}^s c_i^s \right) \max_{t_0 \leq t \leq T} \|f_t^{(s)}(u(t))\| \leq C_2 \Delta t^{s+2}, \quad i = 1, 2, \dots, s, \quad (11.50)$$

where the constant C_2 is given by

$$C_2 = \frac{1 + s\gamma}{(s-1)!} \max_{t_0 \leq t \leq T} \|f_t^{(s)}(u(t))\|, \quad (11.51)$$

and γ is the uniform bound on $a_{ij}(\mathcal{V})$ under the norm $\|\cdot\|_{L^2(\Omega) \leftarrow L^2(\Omega)}$.

Concerning the local error bounds of the Lagrange collocation-type time-stepping integrators (11.39), we have the following result.

Theorem 11.2 *Suppose that $f_t^{(s)} \in L^\infty(0, T; L^2(\Omega))$. Under the local assumptions of $u^n = u(t_n)$, $u'^n = u'(t_n)$, the local error bounds of the time integrators (11.39) satisfy the following inequalities*

$$\begin{aligned} \|u(t_{n+1}) - u^{n+1}\| &\leq 2\Delta t^2 \beta L \sum_{i=1}^s \|\Delta^{ni}\| + \|\delta^{n+1}\|, \\ \|u'(t_{n+1}) - u'^{n+1}\| &\leq 2\Delta t \beta L \sum_{i=1}^s \|\Delta^{ni}\| + \|\delta^{n+1}\|, \end{aligned} \quad (11.52)$$

where the residuals δ^{n+1} , δ'^{n+1} and Δ^{ni} are explicitly represented by (11.42) and (11.49), respectively.

Proof It follows on subtracting (11.39) from (11.41) that

$$\begin{cases} u(t_{n+1}) - u^{n+1} = \Delta t^2 \sum_{i=1}^s b_i(\mathcal{V}) \left(\tilde{f}(t_n + c_i \Delta t) - f(U^{ni}) \right) + \delta^{n+1}, \\ u'(t_{n+1}) - u'^{n+1} = \Delta t \sum_{i=1}^s \bar{b}_i(\mathcal{V}) \left(\tilde{f}(t_n + c_i \Delta t) - f(U^{ni}) \right) + \delta'^{n+1}, \\ u(t_n + c_i \Delta t) - U^{ni} = c_i^2 \Delta t^2 \sum_{j=1}^s a_{ij}(\mathcal{V}) \left(\tilde{f}(t_n + c_j \Delta t) - f(U^{nj}) \right) + \Delta^{ni}, \quad i = 1, 2, \dots, s. \end{cases} \quad (11.53)$$

By taking norms on both sides of the Eq. (11.53) and using Assumption 2, the first two equations yield

$$\begin{aligned} \|u(t_{n+1}) - u^{n+1}\| &\leq \Delta t^2 \sum_{i=1}^s \|b_i(\mathcal{V})\|_{L^2(\Omega) \leftarrow L^2(\Omega)} \|\tilde{f}(t_n + c_i \Delta t) - f(U^{ni})\| + \|\delta^{n+1}\| \\ &\leq \Delta t^2 \beta L \sum_{i=1}^s \|u(t_n + c_i \Delta t) - U^{ni}\| + \|\delta^{n+1}\|, \end{aligned} \quad (11.54)$$

and

$$\begin{aligned} \|u'(t_{n+1}) - u'^{n+1}\| &\leq \Delta t \sum_{i=1}^s \|\bar{b}_i(\mathcal{V})\|_{L^2(\Omega) \leftarrow L^2(\Omega)} \|\tilde{f}(t_n + c_i \Delta t) - f(U^{ni})\| + \|\delta^{n+1}\| \\ &\leq \Delta t \beta L \sum_{i=1}^s \|u(t_n + c_i \Delta t) - U^{ni}\| + \|\delta^{n+1}\|. \end{aligned} \quad (11.55)$$

The last equations of (11.53) give

$$\begin{aligned} \|u(t_n + c_i \Delta t) - U^{ni}\| &\leq c_i^2 \Delta t^2 \sum_{j=1}^s \|\bar{a}_{ij}(\mathcal{V})\|_{L^2(\Omega) \leftarrow L^2(\Omega)} \|\tilde{f}(t_n + c_j \Delta t) - f(U^{nj})\| + \|\Delta^{ni}\| \\ &\leq c_i^2 \Delta t^2 \gamma L \sum_{j=1}^s \|u(t_n + c_j \Delta t) - U^{nj}\| + \|\Delta^{ni}\|, \quad i = 1, 2, \dots, s, \end{aligned} \quad (11.56)$$

where γ is the uniform bound on $a_{ij}(\mathcal{V})$ under the norm $\|\cdot\|_{L^2(\Omega) \leftarrow L^2(\Omega)}$. Summing up the results of (11.56) for i from 1 to s , we obtain

$$\sum_{i=1}^s \|u(t_n + c_i \Delta t) - U^{ni}\| \leq \Delta t^2 \gamma L \sum_{i=1}^s c_i^2 \sum_{j=1}^s \|u(t_n + c_j \Delta t) - U^{nj}\| + \sum_{i=1}^s \|\Delta^{ni}\|. \quad (11.57)$$

If the sufficiently small time stepsize Δt satisfies $\Delta t^2 \gamma L \sum_{i=1}^s c_i^2 \leq \frac{1}{2}$, namely,

$$\Delta t \leq \sqrt{\frac{1}{2\gamma L \sum_{i=1}^s c_i^2}}, \quad (11.58)$$

then we have

$$\sum_{i=1}^s \|u(t_n + c_i \Delta t) - U^{ni}\| \leq 2 \sum_{i=1}^s \|\Delta^{ni}\|. \quad (11.59)$$

Inserting (11.59) into the right-hand sides of inequalities (11.54) and (11.55) yields the following results

$$\|u(t_{n+1}) - u^{n+1}\| \leq 2\Delta t^2 \beta L \sum_{i=1}^s \|\Delta^{ni}\| + \|\delta^{n+1}\|, \quad (11.60)$$

and

$$\|u'(t_{n+1}) - u'^{n+1}\| \leq 2\Delta t \beta L \sum_{i=1}^s \|\Delta^{ni}\| + \|\delta^{n+1}\|. \quad (11.61)$$

The statement of the theorem is proved. \square

Using the estimate of the residuals δ^{n+1} , δ'^{n+1} and Δ^{ni} in (11.43) and (11.50), and inserting them into (11.52), the following corollary clarifies the local error bounds of the Lagrange collocation-type time integrators (11.39).

Corollary 11.1 *Under the condition of Theorem 11.2, the local error bounds of the time integrators (11.39) can be explicitly presented as*

$$\|u(t_{n+1}) - u^{n+1}\| \leq \tilde{C}_1 \Delta t^{s+2} \quad \text{and} \quad \|u'(t_{n+1}) - u'^{n+1}\| \leq \tilde{C}_1 \Delta t^{s+1}, \quad (11.62)$$

where $\tilde{C}_1 = (C_1 + 2C_2 s \beta L \Delta t^2)$, and C_1, C_2 are defined as (11.44) and (11.51), respectively.

Remark 11.3 The weights $b_i(\mathcal{V})$, $\bar{b}_i(\mathcal{V})$ and $a_{ij}(\mathcal{V})$ of the time integrators (11.39) are determined by (11.34), (11.35) and the order conditions (11.48) with appropriate nodes c_i for $i = 1, 2, \dots, s$, respectively.

Remark 11.4 Furthermore, from the analysis of the local error bounds for the time integrators (11.39), it can be observed that there is a term $\max_{0 \leq z \leq 1} |w_s(z)|$ appearing in the constant C_1 . In order to minimise the constant C_1 , it is wise to choose the nodes $\{c_i\}_{i=1}^s$ as the Gauss-Legendre nodes in this chapter.

Remark 11.5 Here, we should point out that the limitation on the time stepsize (11.58) is only a sufficient condition for our theoretical analysis. It is also important for the analysis of the stability and convergence for the proposed fully discrete schemes.

11.4 Spatial Discretisation

The proposed arbitrarily high-order Lagrange collocation-type time-stepping integrators (11.39) are expressed in terms of operator in the infinite dimensional Hilbert space $L^2(\Omega)$. In order to obtain proper numerical schemes, it remains to approximate the differential operator \mathcal{A} with an appropriate differentiation matrix A acting on an M -dimensional space. Furthermore, it is our ideal choice to approximate the differential operator \mathcal{A} by a positive semi-definite matrix A , in such a way that we can achieve a reasonable and rigorous nonlinear stability and convergence analysis. Fortunately, much research has been done on the spatial derivatives of nonlinear system (11.1) with periodic boundary conditions (11.2), from which it is easy to choose a suitable positive semi-definite differential matrix.

In this section, we mainly consider the following two types of spatial discretisations.

1. *Symmetric finite difference (SFD)* (see, e.g. R. Bank, R.L. Graham, J. Stoer, R. Varga, H. Yserentant [5])

where the norm $\|\cdot\|$ is the standard vector 2-norm and $\Delta x = \frac{2\pi}{M}$ is the spatial stepsize. Actually, this energy can be regarded as an approximate energy (a semi-discrete energy) of the original continuous system. Therefore, in the part of the numerical experiments, we will also test the effectiveness of our methods to preserve the semi-discrete energy (11.64).

11.5 The Analysis of Nonlinear Stability and Convergence for the Fully Discrete Scheme

The nonlinear stability and error analysis for the fully discrete scheme over a finite time interval $[t_0, T]$ will be investigated in this section. The main strategy used in this section is the popular energy analysis method. Here, it is noted that, throughout this section $\|\cdot\|$ presents the vector 2-norm or matrix 2-norm (spectral norm).

11.5.1 Analysis of the Nonlinear Stability

In this subsection, we will show the nonlinear stability of our time-stepping integrators (11.39), once the differential operator \mathcal{A} is replaced by a differential matrix A .

Suppose that the perturbed problem of (11.13) is

$$\begin{cases} v''(t) + \mathcal{A}v(t) = f(v(t)), & t \in [t_0, T], \\ v(t_0) = \varphi_1(x) + \tilde{\varphi}_1(x), \quad v'(t_0) = \varphi_2(x) + \tilde{\varphi}_2(x), \end{cases} \quad (11.65)$$

where $\tilde{\varphi}_1(x), \tilde{\varphi}_2(x)$ are perturbation functions. Letting $\eta(t) = v(t) - u(t)$ and subtracting (11.13) from (11.65), we obtain

$$\begin{cases} \eta''(t) + \mathcal{A}\eta(t) = f(v(t)) - f(u(t)), & t \in [t_0, T], \\ \eta(t_0) = \tilde{\varphi}_1(x), \quad \eta'(t_0) = \tilde{\varphi}_2(x). \end{cases} \quad (11.66)$$

In general, the operator \mathcal{A} is approximated by a symmetric, positive semi-definite, differential matrix A in the sense of structure preservation. Then, there exists an orthogonal matrix P and a positive semi-definite diagonal matrix Λ such that

$$A = P^\top \Lambda P.$$

By defining the matrix $D = P^\top \Lambda^{\frac{1}{2}} P$, we obtain the decomposition of matrix A as $A = D^2$. The bounded operator functions $\phi_j(t^2 \mathcal{A})$ are replaced by the matrix

functions $\phi_j(t^2 A)$. Similarly to the boundedness of the operator functions, we also have

$$\|\phi_j(t^2 A)\| = \sqrt{\lambda_{\max}(\phi_j^2(t^2 A))} \leq \gamma_j, \quad j = 0, 1, 2, \dots \tag{11.67}$$

Applying our time-stepping integrators (11.39) to (11.66), we obtain

$$\begin{cases} \eta^{n+1} = \phi_0(V)\eta^n + \Delta t \phi_1(V)\eta^n + \Delta t^2 \sum_{i=1}^s b_i(V)(f(V^{ni}) - f(U^{ni})), \\ \eta^{m+1} = -\Delta t A \phi_1(V)\eta^n + \phi_0(V)\eta^n + \Delta t \sum_{i=1}^s \bar{b}_i(V)(f(V^{ni}) - f(U^{ni})), \\ V^{ni} - U^{ni} = \phi_0(c_i^2 V)\eta^n + c_i \Delta t \phi_1(c_i^2 V)\eta^n + c_i^2 \Delta t^2 \sum_{j=1}^s a_{ij}(V)(f(V^{nj}) - f(U^{nj})), \\ i = 1, 2, \dots, s, \end{cases} \tag{11.68}$$

where $V = \Delta t^2 A$ and $b_i(V)$ and $\bar{b}_i(V)$ are defined by (11.34) and (11.35), respectively. Likewise, we have

$$\|b_i(V)\| \leq \max_{0 \leq z \leq 1} |l_i(z)| \leq \beta \quad \text{and} \quad \|\bar{b}_i(V)\| \leq \max_{0 \leq z \leq 1} |l_i(z)| \leq \beta,$$

which are uniformly bounded.

We rewrite the first two formulae of (11.68) in the following matrix form:

$$\begin{pmatrix} D\eta^{n+1} \\ \eta^{n+1} \end{pmatrix} = \Omega \begin{pmatrix} D\eta^n \\ \eta^n \end{pmatrix} + \sum_{i=1}^s \Delta t \int_0^1 \Omega_i(z) dz \begin{pmatrix} 0 \\ f(U^{ni}) - f(V^{ni}) \end{pmatrix}, \tag{11.69}$$

where

$$\Omega = \begin{pmatrix} \phi_0(V) & \Delta t D\phi_1(V) \\ -\Delta t D\phi_1(V) & \phi_0(V) \end{pmatrix} \tag{11.70}$$

and

$$\Omega_i(z) = l_i(z) \begin{pmatrix} \phi_0((1-z)^2 V) & \Delta t(1-z)D\phi_1((1-z)^2 V) \\ -\Delta t(1-z)D\phi_1((1-z)^2 V) & \phi_0((1-z)^2 V) \end{pmatrix}, \tag{11.71}$$

for $i = 1, \dots, s$. Before the stability analysis, we state a property of the operator-argument functions ϕ_0 and ϕ_1 , and bound the spectral norm of matrices Ω and $\Omega_i(z)$ for $i = 1, 2, \dots, s$.

Lemma 11.1 *The bounded operator-argument functions $\phi_0(A)$ and $\phi_1(A)$ defined by (11.5) satisfy*

$$\phi_0^2(A) + A\phi_1^2(A) = I, \quad (11.72)$$

where A is any positive semi-definite operator or matrix.

Proof Lemma 11.1 can be obtained by a direct calculation based on (11.12). We omit the details of the proof. \square

Lemma 11.2 *Assume that A is a symmetric positive semi-definite matrix and that $V = \Delta t^2 A$. Let the matrices Ω and $\Omega_i(z)$ for $i = 1, 2, \dots, s$ be defined by (11.70) and (11.71), respectively. Then, the spectral norms of matrices Ω and $\Omega_i(z)$ satisfy*

$$\|\Omega\| = 1 \quad \text{and} \quad \|\Omega_i(z)\| = |l_i(z)| \leq \beta, \quad \forall z \in [0, 1], \quad i = 1, 2, \dots, s, \quad (11.73)$$

where β is the uniform bound for the Lagrange basis $|l_i(z)|$.

Proof It is straightforward to verify that

$$\Omega^\top \Omega = \begin{pmatrix} \phi_0^2(V) + V\phi_1^2(V) & 0 \\ 0 & \phi_0^2(V) + V\phi_1^2(V) \end{pmatrix},$$

and

$$\Omega_i^\top(z)\Omega_i(z) = l_i^2(z) \begin{pmatrix} \Omega_i^{11} & 0 \\ 0 & \Omega_i^{22} \end{pmatrix},$$

where

$$\begin{aligned} \Omega_i^{11} &= \phi_0^2((1-z)^2 V) + (1-z)^2 V\phi_1^2((1-z)^2 V), \\ \Omega_i^{22} &= \phi_0^2((1-z)^2 V) + (1-z)^2 V\phi_1^2((1-z)^2 V). \end{aligned}$$

It follows from Lemma 11.1 that

$$\Omega^\top \Omega = I_{2M \times 2M}, \quad \text{and} \quad \Omega_i(z)^\top \Omega_i(z) = l_i^2(z) I_{2M \times 2M}. \quad (11.74)$$

We then have

$$\|\Omega\| = 1 \quad \text{and} \quad \|\Omega_i(z)\| = |l_i(z)| \leq \beta, \quad \forall z \in [0, 1], \quad i = 1, 2, \dots, s.$$

The conclusion of the lemma is proved. \square

Theorem 11.3 *Supposing that the nonlinear function f satisfies Assumption 2 and that the operator \mathcal{A} is approximated by a symmetric positive semi-definite differential matrix A . Then, if the sufficiently small time stepsize Δt satisfies (11.58), we have the following nonlinear stability results*

$$\begin{aligned}\|\eta^n\| &\leq \exp((1 + 4s\beta L)T)(\|\tilde{\varphi}_1\| + \sqrt{\|D\tilde{\varphi}_1\|^2 + \|\tilde{\varphi}_2\|^2}), \\ \|\eta^m\| &\leq \exp((1 + 4s\beta L)T)(\|\tilde{\varphi}_1\| + \sqrt{\|D\tilde{\varphi}_1\|^2 + \|\tilde{\varphi}_2\|^2}),\end{aligned}\quad (11.75)$$

where γ is a uniform bound for $\|a_{ij}(V)\|$.

Proof It follows from taking the l_2 norm on both sides of the first formula (11.68) and (11.69) that

$$\|\eta^{n+1}\| \leq \|\eta^n\| + \Delta t \|\eta^n\| + \Delta t^2 \beta \sum_{i=1}^s (\|f(V^{ni}) - f(U^{ni})\|), \quad (11.76)$$

$$\sqrt{\|D\eta^{n+1}\|^2 + \|\eta^{n+1}\|^2} \leq \sqrt{\|D\eta^n\|^2 + \|\eta^n\|^2} + \Delta t \beta \sum_{i=1}^s (\|f(V^{ni}) - f(U^{ni})\|). \quad (11.77)$$

Then summing up the results, we obtain

$$\begin{aligned}\|\eta^{n+1}\| + \sqrt{\|D\eta^{n+1}\|^2 + \|\eta^{n+1}\|^2} &\leq \|\eta^n\| + \sqrt{\|D\eta^n\|^2 + \|\eta^n\|^2} + \Delta t \|\eta^n\| \\ &\quad + \Delta t(1 + \Delta t)\beta \sum_{i=1}^s (\|f(V^{ni}) - f(U^{ni})\|).\end{aligned}\quad (11.78)$$

Applying Assumption 2 to the right-hand side of the inequality (11.78), we obtain

$$\begin{aligned}\|\eta^{n+1}\| + \sqrt{\|D\eta^{n+1}\|^2 + \|\eta^{n+1}\|^2} &\leq \|\eta^n\| + \sqrt{\|D\eta^n\|^2 + \|\eta^n\|^2} + \Delta t \|\eta^n\| \\ &\quad + \Delta t(1 + \Delta t)\beta L \sum_{i=1}^s (\|V^{ni} - U^{ni}\|).\end{aligned}\quad (11.79)$$

Likewise, it follows from the last equations in (11.68) that

$$\begin{aligned}\|V^{ni} - U^{ni}\| &\leq \|\eta^n\| + c_i \Delta t \|\eta^n\| + c_i^2 \Delta t^2 \sum_{j=1}^s \|a_{ij}(V)\| \cdot \|f(V^{nj}) - f(U^{nj})\| \\ &\leq \|\eta^n\| + c_i \Delta t \|\eta^n\| + c_i^2 \Delta t^2 \gamma L \sum_{j=1}^s \|V^{nj} - U^{nj}\|, \quad i = 1, \dots, s.\end{aligned}\quad (11.80)$$

Then, summing up the results of (11.80) between i from 1 to s , we obtain

$$\sum_{i=1}^s \|V^{ni} - U^{ni}\| \leq \sum_{i=1}^s (\|\eta^n\| + c_i \Delta t \|\eta^n\|) + \Delta t^2 \gamma L \sum_{i=1}^s c_i^2 \sum_{j=1}^s \|V^{nj} - U^{nj}\|. \quad (11.81)$$

This gives

$$\left(1 - \Delta t^2 \gamma L \sum_{i=1}^s c_i^2\right) \sum_{i=1}^s \|V^{ni} - U^{ni}\| \leq \sum_{i=1}^s (\|\eta^n\| + c_i \Delta t \|\eta^n\|). \quad (11.82)$$

If the sufficiently small time stepsize Δt satisfies (11.58), then we have

$$\sum_{i=1}^s \|V^{ni} - U^{ni}\| \leq 2 \sum_{i=1}^s (\|\eta^n\| + c_i \Delta t \|\eta^n\|). \quad (11.83)$$

Inserting (11.83) into (11.79) yields

$$\begin{aligned} & \|\eta^{n+1}\| + \sqrt{\|D\eta^{n+1}\|^2 + \|\eta^{n+1}\|^2} \\ & \leq \|\eta^n\| + \sqrt{\|D\eta^n\|^2 + \|\eta^n\|^2} + \Delta t \|\eta^n\| + 2\Delta t(1 + \Delta t)\beta L \sum_{i=1}^s (\|\eta^n\| + c_i \Delta t \|\eta^n\|). \end{aligned} \quad (11.84)$$

An argument by induction leads to the following result

$$\begin{aligned} \|\eta^{n+1}\| + \sqrt{\|D\eta^{n+1}\|^2 + \|\eta^{n+1}\|^2} & \leq (1 + \Delta t(1 + 4s\beta L))^n (\|\eta^0\| + \sqrt{\|D\eta^0\|^2 + \|\eta^0\|^2}) \\ & \leq \exp(T(1 + 4s\beta L)) (\|\tilde{\varphi}_1\| + \sqrt{\|D\tilde{\varphi}_1\|^2 + \|\tilde{\varphi}_2\|^2}). \end{aligned} \quad (11.85)$$

Thus, the following inequalities are derived

$$\begin{aligned} \|\eta^n\| & \leq \exp((1 + 4s\beta L)T) (\|\tilde{\varphi}_1\| + \sqrt{\|D\tilde{\varphi}_1\|^2 + \|\tilde{\varphi}_2\|^2}), \\ \|\eta^n\| & \leq \exp((1 + 4s\beta L)T) (\|\tilde{\varphi}_1\| + \sqrt{\|D\tilde{\varphi}_1\|^2 + \|\tilde{\varphi}_2\|^2}). \end{aligned} \quad (11.86)$$

The conclusions of the theorem are proved. \square

11.5.2 Convergence of the Fully Discrete Scheme

As is known, the convergence of the classical methods for linear partial differential equations is governed by the Lax equivalence theorem: convergence equals consistency plus stability [33]. However, the Lax equivalence theorem does not directly apply to nonlinear problems.

In this subsection, the error analysis of the fully discrete scheme for nonlinear problems will be discussed. Based on some suitable assumptions of smoothness and spatial discretisation strategies, the original continuous system (11.1) or (11.13) can be discretised as follows:

$$\begin{cases} U''(t) + AU(t) = f(U(t)) + \delta(\Delta x), & t \in [t_0, T], \\ U(t_0) = \varphi_1, \quad U'(t_0) = \varphi_2, \end{cases} \quad (11.87)$$

where A is a positive semi-definite differential matrix,

$$U(t) = (u(x_1, t), u(x_2, t), \dots, u(x_M, t))^T$$

and

$$\varphi_l = (\varphi_l(x_1), \varphi_l(x_2), \dots, \varphi_l(x_M))^T,$$

for $l = 1, 2$.

Here, it should be noted that $\delta(\Delta x)$ is the truncation error produced by approximating the spatial differential operator \mathcal{A} by a positive semi-definite matrix A . For example, if we were to approximate the spatial derivative by the classical fourth-order finite difference method (see, e.g. [5, 39]), then the truncation error $\delta(\Delta x)$ would be $\|\delta(\Delta x)\| = O(\Delta x^4)$.

Applying a time-stepping integrator (11.39) to the semi-discrete system (11.87) yields the following results

$$\left\{ \begin{array}{l} U(t_{n+1}) = \phi_0(V)U(t_n) + \Delta t \phi_1(V)U'(t_n) + \Delta t^2 \sum_{i=1}^s b_i(V)f(U(t_n + c_i \Delta t)) + R^{n+1}, \\ U'(t_{n+1}) = -\Delta t A \phi_1(V)U(t_n) + \phi_0(V)U'(t_n) + \Delta t \sum_{i=1}^s \bar{b}_i(V)f(U(t_n + c_i \Delta t)) + R^{n+1}, \\ U(t_n + c_i \Delta t) = \phi_0(c_i^2 V)U(t_n) + c_i \Delta t \phi_1(c_i^2 V)U'(t_n) + c_i^2 \Delta t^2 \sum_{j=1}^s a_{ij}(V)f(U(t_n + c_j \Delta t)) + R^{ni}, \\ i = 1, 2, \dots, s, \end{array} \right. \tag{11.88}$$

where the truncation errors R^{n+1} , R^{n+1} and R^{ni} can be explicitly represented as

$$R^{n+1} = \frac{\Delta t^{s+2}}{s!} \int_0^1 (1-z)\phi_1((1-z)^2 V)w_s(z)dz f_t^{(s)}(U(t_n + \xi^n \Delta t)) \tag{11.89}$$

$$+ \Delta t^2 \int_0^1 (1-z)\phi_1((1-z)^2 V)\delta(\Delta x)dz, \tag{11.90}$$

$$R^{n+1} = \frac{\Delta t^{s+1}}{s!} \int_0^1 \phi_0((1-z)^2 V)w_s(z)dz f_t^{(s)}(U(t_n + \xi^n \Delta t)) \tag{11.91}$$

$$+ \Delta t \int_0^1 \phi_0((1-z)^2 V)\delta(\Delta x)dz, \tag{11.92}$$

and

$$\begin{aligned} R^{ni} &= \frac{c_i^{s+2} \Delta t^{s+2}}{(s-1)!} \int_0^1 (1-z)\phi_1((1-z)^2 V) \int_0^z f_t^{(s)}(U(t_n + \sigma c_i \Delta t))(z-\sigma)^{s-1} d\sigma dz \\ &\quad - \frac{c_i^2 \Delta t^{s+2}}{(s-1)!} \sum_{j=1}^s a_{ij}(V) \int_0^{c_j} f_t^{(s)}(U(t_n + \sigma \Delta t))(c_j - \sigma)^{s-1} d\sigma \\ &\quad + c_i^2 \Delta t^2 \int_0^1 (1-z)\phi_1((1-z)^2 c_i^2 V)\delta(\Delta x)dz - c_i^2 \Delta t^2 \sum_{j=1}^s a_{ij}(V)\delta(\Delta x). \end{aligned} \tag{11.93}$$

Under some suitable assumptions of smoothness, the truncation errors R^{n+1} , R^{m+1} and R^{ni} satisfy

$$\|R^{n+1}\| \leq C_1 \Delta t^{s+2} + \frac{1}{2} \Delta t^2 \|\delta(\Delta x)\|, \quad \|R^{m+1}\| \leq C_1 \Delta t^{s+1} + \Delta t \|\delta(\Delta x)\|, \tag{11.94}$$

and

$$\|R^{ni}\| \leq C_2 \Delta t^{s+2} + \Delta t^2 (1 + s\gamma) \|\delta(\Delta x)\|, \quad i = 1, 2, \dots, s, \tag{11.95}$$

where the constants C_1 and C_2 are determined by (11.44) and (11.51), respectively.

Omitting the small terms R^{n+1} , R^{m+1} and R^{ni} in (11.88) and using $u_j^n \approx u(x_j, t_n)$, we obtain the following fully discrete scheme

$$\begin{cases} u^{n+1} = \phi_0(V)u^n + \Delta t \phi_1(V)u'^n + \Delta t^2 \sum_{i=1}^s b_i(V)f(U^{ni}), \\ u'^{n+1} = -\Delta t A \phi_1(V)u^n + \phi_0(V)u'^n + \Delta t \sum_{i=1}^s \bar{b}_i(V)f(U^{ni}), \\ U^{ni} = \phi_0(c_i^2 V)u^n + c_i \Delta t \phi_1(c_i^2 V)u'^n + c_i^2 \Delta t^2 \sum_{j=1}^s a_{ij}(V)f(U^{nj}), \quad i = 1, 2, \dots, s. \end{cases} \tag{11.96}$$

We next consider the convergence of the fully discrete scheme (11.96) for non-linear problems. To this end, we denote $e_j^n = u(x_j, t_n) - u_j^n$, $e_j^n = u_t(x_j, t_n) - u_j'^n$ and $E_j^{ni} = u(x_j, t_n + c_i \Delta t) - U_j^{ni}$ for $j = 1, 2, \dots, M$, i.e., $e^n = U(t_n) - u^n$, $e'^n = U'(t_n) - u'^n$ and $E^{ni} = U(t_n + c_i \Delta t) - U^{ni}$. Subtracting (11.96) from (11.88), and on noticing the exact initial conditions, we get a system of error equations expressed in the form

$$\begin{cases} e^{n+1} = \phi_0(V)e^n + \Delta t \phi_1(V)e'^n + \Delta t^2 \sum_{i=1}^s b_i(V)(f(U(t_n + c_i \Delta t)) - f(U^{ni})) + R^{n+1}, \\ e'^{n+1} = -\Delta t A \phi_1(V)e^n + \phi_0(V)e'^n + \Delta t \sum_{i=1}^s \bar{b}_i(V)(f(U(t_n + c_i \Delta t)) - f(U^{ni})) + R^{n+1}, \\ E^{ni} = \phi_0(c_i^2 V)e^n + c_i \Delta t \phi_1(c_i^2 V)e'^n + c_i^2 \Delta t^2 \sum_{j=1}^s a_{ij}(V)(f(U(t_n + c_i \Delta t)) - f(U^{nj})) + R^{ni}, \\ i = 1, 2, \dots, s, \end{cases} \tag{11.97}$$

with the initial conditions $e^0 = 0$, $e'^0 = 0$.

In what follows, we quote the following discrete Gronwall inequality, which plays an important role in the convergence analysis for the fully discrete scheme.

Lemma 11.3 (See, e.g. [48]) *Let μ be positive and a_k, b_k ($k = 0, 1, 2, \dots$) be nonnegative and satisfy*

$$a_k \leq (1 + \mu \Delta t)a_{k-1} + \Delta t b_k, \quad k = 1, 2, 3, \dots,$$

then

$$a_k \leq \exp(\mu k \Delta t) \left(a_0 + \Delta t \sum_{m=1}^k b_m \right), \quad k = 1, 2, 3, \dots$$

Theorem 11.4 *Under the Assumptions 1 and 2, and suppose that $u(x, t)$ satisfies some suitable assumptions on smoothness. If the time stepsize Δt is sufficiently small and satisfies (11.58), then there exists a constant C such that*

$$\begin{aligned} \|e^n\| &\leq CT \exp((1 + 4s\beta L)T) (\Delta t^s + \|\delta(\Delta x)\|), \\ \|e^n\| &\leq CT \exp((1 + 4s\beta L)T) (\Delta t^s + \|\delta(\Delta x)\|), \end{aligned} \tag{11.98}$$

where C is a constant independent of n , Δt and Δx .

Proof The first two equations of the error system (11.97) can be rewritten in the compact form

$$\begin{pmatrix} De^{n+1} \\ e^{n+1} \end{pmatrix} = \Omega \begin{pmatrix} De^n \\ e^n \end{pmatrix} + \Delta t \sum_{i=1}^s \int_0^1 \Omega_i(z) dz \begin{pmatrix} 0 \\ f(U(t_n + c_i \Delta t)) - f(U^{ni}) \end{pmatrix} + \begin{pmatrix} DR^{n+1} \\ R^{n+1} \end{pmatrix}, \tag{11.99}$$

where Ω and $\Omega_i(z)$ are defined by (11.70) and (11.71), respectively.

It follows from taking the l_2 norm on both sides of the first formula (11.97) and (11.99) that

$$\begin{aligned} \|e^{n+1}\| &\leq \|e^n\| + \Delta t \|e^n\| + \Delta t^2 \beta \sum_{i=1}^s \|f(U(t_n + c_i \Delta t)) - f(U^{ni})\| + \|R^{n+1}\|, \\ \sqrt{\|De^{n+1}\|^2 + \|e^{n+1}\|^2} &\leq \sqrt{\|De^n\|^2 + \|e^n\|^2} + \Delta t \beta \sum_{i=1}^s \|f(U(t_n + c_i \Delta t)) - f(U^{ni})\| \\ &\quad + \sqrt{\|DR^{n+1}\|^2 + \|R^{n+1}\|^2}. \end{aligned} \tag{11.100}$$

Then, summing up the results of (11.100) and using the Assumption 2, we obtain

$$\begin{aligned} \|e^{n+1}\| + \sqrt{\|De^{n+1}\|^2 + \|e^{n+1}\|^2} &\leq \|e^n\| + \Delta t \|e^n\| + \sqrt{\|De^n\|^2 + \|e^n\|^2} \\ &\quad + \Delta t (1 + \Delta t) \beta L \sum_{i=1}^s \|E^{ni}\| + \|R^{n+1}\| + \sqrt{\|DR^{n+1}\|^2 + \|R^{n+1}\|^2}. \end{aligned} \tag{11.101}$$

Likewise, taking the l_2 norm on both sides of the last equations of the error system (11.97) yields

$$\|E^{ni}\| \leq \|e^n\| + c_i \Delta t \|e^n\| + c_i^2 \Delta t^2 \gamma L \sum_{i=1}^s \|E^{ni}\| + \|R^{ni}\|, \quad i = 1, 2, \dots, s. \tag{11.102}$$

Summing the results of (11.102) for i from 1 to s gives

$$\sum_{i=1}^s \|E^{ni}\| \leq \sum_{i=1}^s (\|e^n\| + c_i \Delta t \|e^n\| + \|R^{ni}\|) + \Delta t^2 \gamma L \sum_{i=1}^s c_i^2 \sum_{j=1}^s \|E^{nj}\|. \quad (11.103)$$

Under the condition (11.58), we obtain

$$\sum_{i=1}^s \|E^{ni}\| \leq 2 \sum_{i=1}^s (\|e^n\| + c_i \Delta t \|e^n\|) + 2 \sum_{i=1}^s \|R^{ni}\|. \quad (11.104)$$

Inserting (11.104) into (11.101) yields

$$\begin{aligned} \|e^{n+1}\| + \sqrt{\|De^{n+1}\|^2 + \|e^{n+1}\|^2} &\leq \|e^n\| + \Delta t \|e^n\| + \sqrt{\|De^n\|^2 + \|e^n\|^2} \\ &+ 2\Delta t(1 + \Delta t)\beta L \sum_{i=1}^s (\|e^n\| + c_i \Delta t \|e^n\|) + \|R^{n+1}\| + \sqrt{\|DR^{n+1}\|^2 + \|R^{n+1}\|^2} \\ &+ 2\Delta t(1 + \Delta t)\beta L \sum_{i=1}^s \|R^{ni}\|. \end{aligned} \quad (11.105)$$

It follows from the inequality (11.105) that

$$\begin{aligned} \|e^{n+1}\| + \sqrt{\|De^{n+1}\|^2 + \|e^{n+1}\|^2} &\leq (1 + \Delta t(1 + 4s\beta L))(\|e^n\| + \sqrt{\|De^n\|^2 + \|e^n\|^2}) \\ &+ \|R^{n+1}\| + \sqrt{\|DR^{n+1}\|^2 + \|R^{n+1}\|^2} + 2\Delta t(1 + \Delta t)\beta L \sum_{i=1}^s \|R^{ni}\|. \end{aligned} \quad (11.106)$$

We note that the truncation errors R^{n+1} , R^{n+1} and R^{ni} satisfy (11.94) and (11.95), respectively. Then, there exists a constant C satisfying

$$\|R^{n+1}\| + \sqrt{\|DR^{n+1}\|^2 + \|R^{n+1}\|^2} + 2\Delta t(1 + \Delta t)\beta L \sum_{i=1}^s \|R^{ni}\| \leq C\Delta t(\Delta t^s + \|\delta(\Delta x)\|). \quad (11.107)$$

Applying the discrete Gronwall inequality (Lemma 11.3) to (11.106) yields

$$\begin{aligned} \|e^n\| + \sqrt{\|De^n\|^2 + \|e^n\|^2} &\leq \exp(n\Delta t(1 + 4s\beta L)) \left(\|e^0\| + \sqrt{\|De^0\|^2 + \|e^0\|^2} \right. \\ &\quad \left. + Cn\Delta t(\Delta t^s + \|\delta(\Delta x)\|) \right). \end{aligned} \quad (11.108)$$

Therefore, we obtain the following estimates:

$$\begin{aligned} \|e^n\| &\leq CT \exp((1 + 4s\beta L)T) (\Delta t^s + \|\delta(\Delta x)\|), \\ \|e^n\| &\leq CT \exp((1 + 4s\beta L)T) (\Delta t^s + \|\delta(\Delta x)\|). \end{aligned} \quad (11.109)$$

The conclusions of the theorem are confirmed. \square

11.5.3 The Convergence of the Fixed-Point Iteration

The previous subsections derived and analysed the fully discrete scheme. However, the scheme (11.96) is implicit in general. Therefore, iteration is required in practical computations. Fortunately, a wide range of iterative methods (see, e.g. [34, 42, 52]) can be chosen for (11.96). Here, we will use the fixed-point iteration for the implicit scheme and analyse its convergence.

Actually, the iteration is needed only for the computation of the internal stages. The iterative procedure of the fixed-point iteration for (11.96) can be read as

$$\begin{cases} U_{[0]}^{ni} = \phi_0(c_i^2 V)u^n + c_i \Delta t \phi_1(c_i^2 V)u^n, \\ U_{[m+1]}^{ni} = \phi_0(c_i^2 V)u^n + c_i \Delta t \phi_1(c_i^2 V)u^n + c_i^2 \Delta t^2 \sum_{j=1}^s a_{ij}(V) f(U_{[m]}^{nj}), \\ i = 1, 2, \dots, s, \quad m = 0, 1, 2, \dots, \end{cases} \quad (11.110)$$

and

$$\begin{cases} u^{n+1} = \phi_0(V)u^n + \Delta t \phi_1(V)u^n + \Delta t^2 \sum_{i=1}^s b_i(V) f(U^{ni}), \\ u^{m+1} = -\Delta t A \phi_1(V)u^n + \phi_0(V)u^n + \Delta t \sum_{i=1}^s \bar{b}_i(V) f(U^{ni}). \end{cases} \quad (11.111)$$

Theorem 11.5 *Let the nonlinear function f satisfy the Assumption 2. If the time stepsize Δt satisfies the condition (11.58), the iteration procedure determined by (11.110) and (11.111) is convergent.*

Proof According to Assumption 2 and (11.110), the following inequalities can be obtained

$$\begin{aligned} \|U_{[m+1]}^{ni} - U_{[m]}^{ni}\| &\leq c_i^2 \Delta t^2 \sum_{j=1}^s \|a_{ij}(V)\| \cdot \|f(U_{[m]}^{nj}) - f(U_{[m-1]}^{nj})\| \\ &\leq \Delta t^2 \gamma L c_i^2 \sum_{j=1}^s \|U_{[m]}^{nj} - U_{[m-1]}^{nj}\|, \quad i = 1, 2, \dots, s. \end{aligned} \quad (11.112)$$

Then, summing over i in (11.112) yields

$$\sum_{i=1}^s \|U_{[m]}^{ni} - U_{[m-1]}^{ni}\| \leq \Delta t^2 \gamma L \sum_{i=1}^s c_i^2 \sum_{j=1}^s \|U_{[m]}^{nj} - U_{[m-1]}^{nj}\|. \quad (11.113)$$

An argument by induction then gives the following result:

$$\sum_{i=1}^s \|U_{[m]}^{ni} - U_{[m-1]}^{ni}\| \leq \left(\Delta t^2 \gamma L \sum_{i=1}^s c_i^2\right)^m \sum_{i=1}^s \|U_{[1]}^{ni} - U_{[0]}^{ni}\|. \quad (11.114)$$

The limitation of the time stepsize (11.58) leads to

$$\lim_{m \rightarrow +\infty} \left(\sum_{i=1}^s \|U_{[m]}^{ni} - U_{[m-1]}^{ni}\| \right) \leq \lim_{m \rightarrow +\infty} \frac{1}{2^m} \sum_{i=1}^s \|U_{[1]}^{ni} - U_{[0]}^{ni}\| = 0. \quad (11.115)$$

Therefore, the iterative procedure (11.110)–(11.111) is convergent.

11.6 The Application to Two-dimensional Dirichlet or Neumann Boundary Problems

The problem considered in (11.1) is the one-dimensional case, and is equipped with the special periodic boundary conditions (11.2). However, our approach can be extended to the considerably more important high-dimensional Klein–Gordon equations. The computational methodology developed in this chapter is very useful and has potential applications in solving more sophisticated multi-dimensional solitary wave equations. In this section, we mainly concentrate on discussing the application of our time-stepping schemes (11.39) to the two-dimensional nonlinear Klein–Gordon equations equipped with Dirichlet or Neumann boundary conditions. There has been a considerable amount of recent discussions on the computation of 2D sine–Gordon type solitons, in particular via different finite difference and finite element methods, splitting algorithms and predictor–corrector schemes (see, e.g. [2, 4, 11, 12, 19, 45]).

The two-dimensional nonlinear Klein–Gordon equation under consideration is expressed by

$$\begin{cases} u_{tt} - a^2(u_{xx} + u_{yy}) = f(u), & (x, y) \in \Omega, \quad t_0 < t \leq T, \\ u(x, y, t_0) = \varphi_0(x, y), \quad u_t(x, y, t_0) = \varphi_1(x, y), & (x, y) \in \bar{\Omega}, \end{cases} \quad (11.116)$$

where $f(u)$ is a nonlinear function of u chosen as the negative derivative of a potential energy $V(u)$. Here, we suppose that the 2D problem (11.116) is defined on the spatial domain $\Omega = (0, \pi) \times (0, \pi)$ and supplemented with homogenous *Dirichlet boundary conditions*:

$$u(0, y, t) = u(\pi, y, t) = 0, \quad u(x, 0, t) = u(x, \pi, t) = 0, \quad \forall t \in [t_0, T], \quad (11.117)$$

and homogenous *Neumann boundary conditions*:

$$\left. \frac{\partial u}{\partial x} \right|_{x=0,\pi} = 0, \quad \left. \frac{\partial u}{\partial y} \right|_{y=0,\pi} = 0, \quad \forall t \in [t_0, T]. \quad (11.118)$$

For an abstract formulation of the problem (11.116), the linear differential operator \mathcal{A} now should be defined as

$$(\mathcal{A}v)(x, y) = -a^2(\partial_x^2 + \partial_y^2)v(x, y). \quad (11.119)$$

Likewise, \mathcal{A} is an unbounded symmetric and positive semi-definite operator but not defined for every $v \in L^2(\Omega)$. For our further analysis, the inner product of the space $L^2(\Omega)$ is defined as

$$(u, v) = \int_0^\pi \int_0^\pi u(x, y)v(x, y)dx dy. \quad (11.120)$$

In order to model the homogenous Dirichlet and Neumann boundary conditions, the operator \mathcal{A} should be defined on different function spaces respectively. In what follows, we will analyse the the two-dimensional case.

11.6.1 2D Klein–Gordon Equation with Dirichlet Boundary Conditions

The operator \mathcal{A} is defined on the following domain

$$D(\mathcal{A}) = H^2(\Omega) \cap H_0^1(\Omega). \quad (11.121)$$

In this case, the functions $\sin(mx + ny)$ are orthogonal eigenfunctions of the operator \mathcal{A} corresponding to the eigenvalues $a^2(m^2 + n^2)$, $m, n = 1, 2, \dots$. The functions of the operator \mathcal{A} can be defined as:

$$\phi_j(t\mathcal{A})v(x, y) = \sum_{m=1}^{\infty} \sum_{n=1}^{\infty} \hat{v}_{m,n} \phi_j(a^2(m^2 + n^2)t) \sin(mx + ny) \quad (11.122)$$

for $v(x, y) = \sum_{m=1}^{\infty} \sum_{n=1}^{\infty} \hat{v}_{m,n} \sin(mx + ny) \in L^2(\Omega)$, where all $\hat{v}_{m,n}$ are the Fourier coefficients of $v(x, y)$. In order to show the operator functions $\phi_j(t\mathcal{A})$ for any $\forall t \in [t_0, T]$ are bounded, we will characterise the L^2 norm in the frequency space as

$$\|v\|^2 = \int_0^\pi \int_0^\pi |v(x, y)|^2 dx dy = \frac{\pi^2}{4} \sum_{m=1}^{\infty} \sum_{n=1}^{\infty} |\hat{v}_{m,n}|^2. \quad (11.123)$$

Lemma 11.4 *The functions of the operator \mathcal{A} defined by (11.122) are bounded operator under the norm $\|\cdot\|_{L^2(\Omega) \leftarrow L^2(\Omega)}$, i.e.,*

$$\|\phi_j(t\mathcal{A})\|_{L^2(\Omega) \leftarrow L^2(\Omega)} \leq \gamma_j, \quad (11.124)$$

where γ_j are the bounds of the functions $\phi_j(x)$ for $j = 0, 1, 2, \dots$ for $x \geq 0$, respectively.

Proof For any function $u(x, y) \in L^2(\Omega)$, its Fourier series can be expressed as

$$u(x, y) = \sum_{m=1}^{\infty} \sum_{n=1}^{\infty} \hat{u}_{m,n} \sin(mx + ny).$$

Considering the definition of the norm, we obtain

$$\|\phi_j(t\mathcal{A})u\|^2 = \frac{\pi^2}{4} \sum_{m=1}^{\infty} \sum_{n=1}^{\infty} |\hat{u}_{m,n}|^2 |\phi_j(a^2(m^2 + n^2)t)|^2 \leq \sup_{t \geq 0} |\phi_j(a^2(m^2 + n^2)t)|^2 \cdot \|u\|^2 \leq \gamma_j^2 \|u\|^2.$$

Thus, we deduce the following inequality

$$\|\phi_j(t\mathcal{A})\|_{L^2(\Omega) \leftarrow L^2(\Omega)}^2 = \sup_{\|u\| \neq 0} \frac{\|\phi_j(t\mathcal{A})u\|^2}{\|u\|^2} \leq \gamma_j^2, \quad j = 0, 1, 2, \dots$$

The conclusion of the lemma is proved. \square

The following lemma shows that the operator functions $\phi_j(t\mathcal{A})$ for $j = 0, 1, 2, \dots$ are symmetric.

Lemma 11.5 *The bounded operator functions $\phi_j(t\mathcal{A})$ for $j = 0, 1, 2, \dots$ are symmetric operators with respect to the inner product (11.120).*

Proof For any functions $u(x, y), v(x, y) \in L^2(\Omega)$, we have

$$\begin{aligned} (\phi_j(t\mathcal{A})u, v) &= \int_0^\pi \int_0^\pi \phi_j(t\mathcal{A})u(x, y)v(x, y) dx dy \\ &= \frac{\pi^2}{4} \sum_{m=1}^{\infty} \sum_{n=1}^{\infty} \hat{u}_{m,n} \hat{v}_{m,n} \phi_j(a^2(m^2 + n^2)t), \end{aligned}$$

and

$$\begin{aligned} (u, \phi_j(t\mathcal{A})v) &= \int_0^\pi \int_0^\pi u(x, y)\phi_j(t\mathcal{A})v(x, y) dx dy \\ &= \frac{\pi^2}{4} \sum_{m=1}^{\infty} \sum_{n=1}^{\infty} \hat{u}_{m,n} \hat{v}_{m,n} \phi_j(a^2(m^2 + n^2)t). \end{aligned}$$

Hence, we have

$$(\phi_j(t\mathcal{A})u, v) = (u, \phi_j(t\mathcal{A})v), \quad j = 0, 1, 2, \dots$$

The symmetry of the bounded operator functions is proved. \square

11.6.2 2D Klein–Gordon Equation with Neumann Boundary Conditions

In this case, we define the operator \mathcal{A} on the domain

$$D(\mathcal{A}) = \{v \in H^2(\Omega) : v_x = 0, v_y = 0, (x, y) \in \partial\Omega\}. \quad (11.125)$$

The orthogonal eigenfunctions of the operator \mathcal{A} are $\cos(mx + ny)$, and the corresponding eigenvalues are $a^2(m^2 + n^2)$ for $m, n = 0, 1, 2, \dots$. We define the operator functions of \mathcal{A} as:

$$\phi_j(t\mathcal{A})v(x, y) = \sum_{m=0}^{\infty} \sum_{n=0}^{\infty} \hat{v}_{m,n} \phi_j(a^2(m^2 + n^2)t) \cos(mx + ny), \quad (11.126)$$

for $v(x, y) = \sum_{m=0}^{\infty} \sum_{n=0}^{\infty} \hat{v}_{m,n} \cos(mx + ny) \in L^2(\Omega)$, where $\hat{v}_{m,n}$ are the Fourier coefficients of $v(x, y)$. Similarly, the L^2 norm can be characterized in the frequency space by

$$\|v\|^2 = \int_0^\pi \int_0^\pi |v(x, y)|^2 dx dy = \frac{\pi^2}{4} \sum_{m=0}^{\infty} \sum_{n=0}^{\infty} |\hat{v}_{m,n}|^2. \quad (11.127)$$

In what follows, we show the boundedness of the operator functions $\phi_j(t\mathcal{A})$ for $j = 0, 1, 2, \dots$ by the following Lemma.

Lemma 11.6 *The functions of the operator \mathcal{A} defined by (11.126) are bounded operator under the norm $\|\cdot\|_{L^2(\Omega) \leftarrow L^2(\Omega)}$, i.e.,*

$$\|\phi_j(t\mathcal{A})\|_{L^2(\Omega) \leftarrow L^2(\Omega)} \leq \gamma_j, \quad (11.128)$$

where γ_j are the bounds of the functions $\phi_j(x)$, $j = 0, 1, 2, \dots$ for $x \geq 0$, respectively.

Proof For any function $u(x, y) \in L^2(\Omega)$, its Fourier series can be expressed by

$$u(x, y) = \sum_{m=0}^{\infty} \sum_{n=0}^{\infty} \hat{u}_{m,n} \cos(mx + ny).$$

Considering the definition of the norm, we obtain

$$\|\phi_j(t\mathcal{A})u\|^2 = \frac{\pi^2}{4} \sum_{m=0}^{\infty} \sum_{n=0}^{\infty} |\hat{u}_{m,n}|^2 |\phi_j(a^2(m^2+n^2)t)|^2 \leq \sup_{t \geq 0} |\phi_j(a^2(m^2+n^2)t)|^2 \cdot \|u\|^2 \leq \gamma_j^2 \|u\|^2.$$

Hence, we deduce the following inequality

$$\|\phi_j(t\mathcal{A})\|_{L^2(\Omega) \leftarrow L^2(\Omega)}^2 = \sup_{\|u\| \neq 0} \frac{\|\phi_j(t\mathcal{A})u\|^2}{\|u\|^2} \leq \gamma_j^2, \quad j = 0, 1, 2, \dots$$

The conclusion of the lemma is proved. \square

Similarly, the following lemma shows that the operator functions $\phi_j(t\mathcal{A})$ are symmetric for $j = 0, 1, 2, \dots$

Lemma 11.7 *The bounded operator functions $\phi_j(t\mathcal{A})$ for $j = 0, 1, 2, \dots$ are symmetric operators with respect to the inner product (11.120).*

Proof For any functions $u(x, y), v(x, y) \in L^2(\Omega)$, we have

$$\begin{aligned} (\phi_j(t\mathcal{A})u, v) &= \int_0^\pi \int_0^\pi \phi_j(t\mathcal{A})u(x, y)v(x, y) dx dy \\ &= \frac{\pi^2}{4} \sum_{m=0}^{\infty} \sum_{n=0}^{\infty} \hat{u}_{m,n} \hat{v}_{m,n} \phi_j(a^2(m^2+n^2)t), \end{aligned}$$

and

$$\begin{aligned} (u, \phi_j(t\mathcal{A})v) &= \int_0^\pi \int_0^\pi u(x, y)\phi_j(t\mathcal{A})v(x, y) dx dy \\ &= \frac{\pi^2}{4} \sum_{m=0}^{\infty} \sum_{n=0}^{\infty} \hat{u}_{m,n} \hat{v}_{m,n} \phi_j(a^2(m^2+n^2)t). \end{aligned}$$

We then have

$$(\phi_j(t\mathcal{A})u, v) = (u, \phi_j(t\mathcal{A})v), \quad j = 0, 1, 2, \dots$$

The statement of the theorem is confirmed. \square

11.6.3 Abstract ODE Formulation and Spatial Discretisation

Similarly to the one dimensional periodic boundary problem (11.1)–(11.2), by defining $u(t)$ as the function that maps (x, y) to $u(x, y, t)$:

$$u(t) = [(x, y) \mapsto u(x, y, t)],$$

we can formulate the two-dimensional problem (11.116) equipped with the Dirichlet boundary conditions (11.121) or Neumann boundary conditions (11.125) as the following abstract ODE on the Hilbert space $L^2(\Omega)$:

$$\begin{cases} u''(t) + \mathcal{A}u(t) = f(u(t)), \\ u(t_0) = \varphi_1(x, y), \quad u'(t_0) = \varphi_2(x, y). \end{cases} \tag{11.129}$$

Theorem 11.6 *The solution of the abstract ODE (11.129) and its derivative satisfy*

$$\begin{cases} u(t) = \phi_0((t - t_0)^2 \mathcal{A})u(t_0) + (t - t_0)\phi_1((t - t_0)^2 \mathcal{A})u'(t_0) \\ \quad + \int_{t_0}^t (t - \zeta)\phi_1((t - \zeta)^2 \mathcal{A})f(u(\zeta))d\zeta, \\ u'(t) = -(t - t_0)\mathcal{A}\phi_1((t - t_0)^2 \mathcal{A})u(t_0) + \phi_0((t - t_0)^2 \mathcal{A})u'(t_0) \\ \quad + \int_{t_0}^t \phi_0((t - \zeta)^2 \mathcal{A})f(u(\zeta))d\zeta, \end{cases} \tag{11.130}$$

where $\phi_0((t - t_0)^2 \mathcal{A})$, $\phi_1((t - t_0)^2 \mathcal{A})$ are bounded functions of the operator \mathcal{A} for $\forall t \in [t_0, T]$.

Based on the above analysis, it is straightforward to extend our time-stepping integrators (11.39) to two-dimensional nonlinear Klein–Gordon equations with Dirichlet or Neumann boundary conditions. Moreover, we note that the orthogonal eigenfunctions of the operator \mathcal{A} for Dirichlet and Neumann boundary problems are $\sin(mx) \sin(ny)$ and $\cos(mx) \cos(ny)$, respectively. In order to reduce the computation caused by the spatial discretisation, we focus much more on choosing Fourier spectral methods. The numerous related researches on the *discrete Fast Cosine / Sine Transformation* have been widely studied in the literature (see, e.g. [14–16, 43]). The corresponding spatial discretisation methods are the *discrete Fast Sine Transformation* for the underlying Dirichlet boundary problem, and the *discrete Fast Cosine Transformation* for the underlying Neumann boundary case.

11.7 Numerical Experiments

In this section, we derive three practical time integrators and illustrate the numerical results for one dimensional Klein–Gordon equation with periodic boundary conditions and two-dimensional sine–Gordon with homogenous Dirichlet or Neumann boundary conditions. It is clear that our time integrators (11.39) are determined by (11.34), (11.35) and (11.48) with appropriate nodes c_i for $i = 1, 2, \dots, s$. Moreover, we note from our error analysis that there is a term $\max_{0 \leq z \leq 1} |w_s(z)|$ involved in

the constant C_1 . In order to minimise the constant C_1 , here and in the following, we choose Gauss-Legendre nodes.

In the first example, we choose the two-point Gauss-Legendre nodes,

$$c_1 = \frac{3 - \sqrt{3}}{6}, \quad c_2 = \frac{3 + \sqrt{3}}{6}, \quad (11.131)$$

and the corresponding time integrator determined by (11.34), (11.35) and (11.48) is denoted by **GLC2**.

For the second example, the following three-point Gauss-Legendre nodes

$$c_1 = \frac{5 - \sqrt{15}}{10}, \quad c_2 = \frac{1}{2}, \quad c_3 = \frac{5 + \sqrt{15}}{10}, \quad (11.132)$$

together with (11.34), (11.35) and (11.48) determine the three-point time integrator which is denoted by **GLC3**.

For the third example, we take the four-point Gauss-Legendre nodes

$$\begin{aligned} c_1 &= \frac{1 - \sqrt{\frac{15+2\sqrt{30}}{35}}}{2}, & c_2 &= \frac{1 - \sqrt{\frac{15-2\sqrt{30}}{35}}}{2}, \\ c_3 &= \frac{1 + \sqrt{\frac{15-2\sqrt{30}}{35}}}{2}, & c_4 &= \frac{1 + \sqrt{\frac{15+2\sqrt{30}}{35}}}{2}, \end{aligned} \quad (11.133)$$

and denote the corresponding time integrator determined by (11.34), (11.35) and (11.48) by **GLC4**.

For comparison, in what follows, we briefly describe a collection of classical finite difference and the method-of-lines approximations of the nonlinear Klein–Gordon equation. The methods are listed below:

1. *The standard finite difference schemes* (see, e.g. [9, 25, 48])

Let u_j^n be the approximation of $u(x_j, t_n)$ ($j = 0, 1, \dots, M, n = 0, 1, \dots, N$) and introduce the finite difference discretisation operators

$$\delta_t^2 u_j^n = \frac{u_j^{n+1} - 2u_j^n + u_j^{n-1}}{\Delta t^2} \quad \text{and} \quad \delta_x^2 u_j^n = \frac{u_{j+1}^n - 2u_j^n + u_{j-1}^n}{\Delta x^2}.$$

Here, we consider three frequently used *finite difference schemes* to discretise the problem (11.1)–(11.2) as follows:

- Explicit finite difference (*Expt-FD*) scheme

$$\delta_t^2 u_j^n - a^2 \delta_x^2 u_j^n = f(u_j^n);$$

- Semi-implicit finite difference (*Simplt-FD*) scheme

$$\delta_t^2 u_j^n - \frac{a^2}{2} (\delta_x^2 u_j^{n+1} + \delta_x^2 u_j^{n-1}) = f(u_j^n);$$

- Compact finite difference (*Compt-FD*) scheme

$$\left(I + \frac{\Delta x^2}{12} \delta_x^2\right) \delta_t^2 u_j^n - \frac{a^2}{2} (\delta_x^2 u_j^{n+1} + \delta_x^2 u_j^{n-1}) = \left(I + \frac{\Delta x^2}{12} \delta_x^2\right) f(u_j^n).$$

2. The method-of-lines schemes

Firstly, we approximate the spatial differential operator \mathcal{A} to obtain a semi-discrete system of the form

$$u''(t) + Au(t) = f(u(t)), \quad (11.134)$$

where A is a symmetric and positive semi-definite matrix. Then, we use an ODE solver to deal with the semi-discrete system. There are many different ODE solvers for the semi-discrete system (11.134). Here, the time integrators selected for comparisons are:

- GAS2s4: the two-stage Gauss time integration method of order four presented in [28];
- LIIIB4s6: the Labatto IIIB method of order six presented in [28];
- IRKN2s4: the two-stage implicit symplectic Runge-Kutta-Nyström (IRKN) method of order four derived in [51];
- IRKN3s6: the three-stage implicit symplectic Runge-Kutta-Nyström (IRKN) method of order six derived in [51];
- ERKN3s4: the three-stage extended Runge-Kutta-Nyström (ERKN) time integration method of order four for second order ODEs proposed in [54];
- SMMERKN5s5: the five-stage explicit symplectic multi-frequency and multi-dimensional extended Runge-Kutta-Nyström (ERKN) method of order five with some small residuals for second order ODEs proposed in [55].

It is noted that we use fixed-point iteration for all of the implicit time integration methods in our numerical experiments. We set the error tolerance as 10^{-15} , and put the maximum iteration number $m = 1000$ in each iteration procedure. Here, it should be pointed out that, if the error produced by a method is too large for some time stepsize Δt , then the corresponding point will not be plotted in the figure.

All computations in the numerical experiments are carried out by using MATLAB 2011b on the the computer Lenovo ThinkCentre M8300t (CPU: Intel (R) Core (TM) i5-2400 CPU @ 3.10 GHz, Memory: 8 GB, Os: Microsoft Windows 7 with 64 bit).

11.7.1 One-dimensional Problem with Periodic Boundary Conditions

Problem 11.1 We consider the sine–Gordon equation

$$\frac{\partial^2 u}{\partial t^2}(x, t) - \frac{\partial^2 u}{\partial x^2}(x, t) = -\sin(u(x, t)), \quad (11.135)$$

on the region $-20 \leq x \leq 20$ and $0 \leq t \leq T$, subject to the initial conditions

$$u(x, 0) = 0, \quad u_t(x, 0) = 4\operatorname{sech}\left(x/\sqrt{1+c^2}\right)/\sqrt{1+c^2},$$

where $\kappa = 1/\sqrt{1+c^2}$. The exact solution of this problem is given by

$$u(x, t) = 4 \arctan\left(c^{-1} \sin(ct/\sqrt{1+c^2})\operatorname{sech}(x/\sqrt{1+c^2})\right).$$

This problem is known as the breather solution of the sine–Gordon equation (see, e.g. [39]), and represents a pulse-type structure of a soliton. The parameter c is the velocity and we choose $c = 0.5$. The potential function is $V(u) = 1 - \cos(u)$.

In Figs. 11.1 and 11.2, we integrate the sine–Gordon equation (11.135) over the region $(x, t) \in [-20, 20] \times [0, 100]$ using the time integrator **GLC4** coupled with the eighth-order symmetric finite difference (SFD) method and the Fourier spectral collocation (FSC) method. The graphs of the errors are shown in Figs. 11.1 and 11.2 with the time stepsize $\Delta t = 0.01$ and several different values of M . The numerical results demonstrate the accuracy of the spatial discretisation, and also indicate that the Fourier spectral collocation method is much better to discretise the spatial derivative than the eighth-order finite difference method. Therefore, it is evident that the Fourier spectral collocation method is the best choice to discretise the spatial variable for this problem.

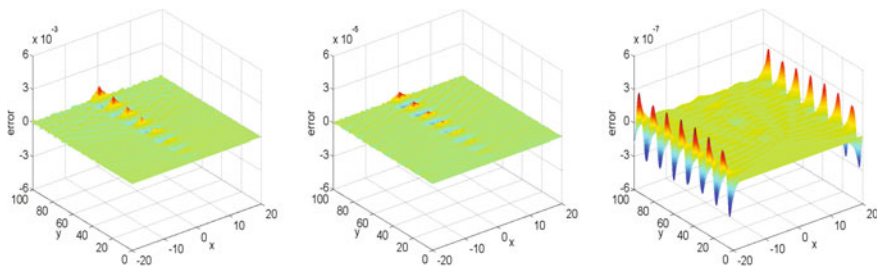


Fig. 11.1 The graphs of errors for the sine–Gordon equation obtained by combining the time integrator GLC4 with eighth-order finite difference spatial discretisation for the time stepsize $\Delta t = 0.01$ and several values of $M = 100$ (left), 200 (middle), and 400 (right)

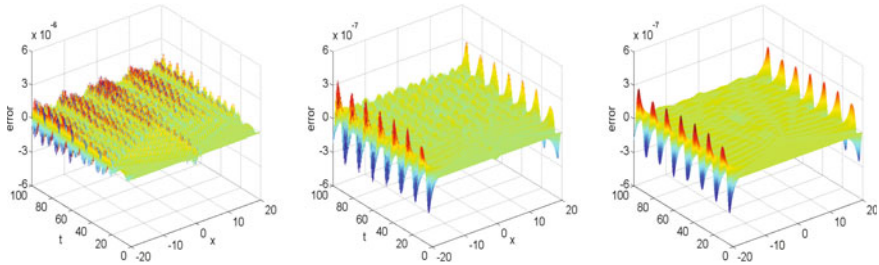


Fig. 11.2 The errors produced by combining the time integrator GLC4 with spatial discretisation by the Fourier spectral method for the time stepsize $\Delta t = 0.01$ and several values of $M = 100$ (left), 120 (middle), and 200 (right)

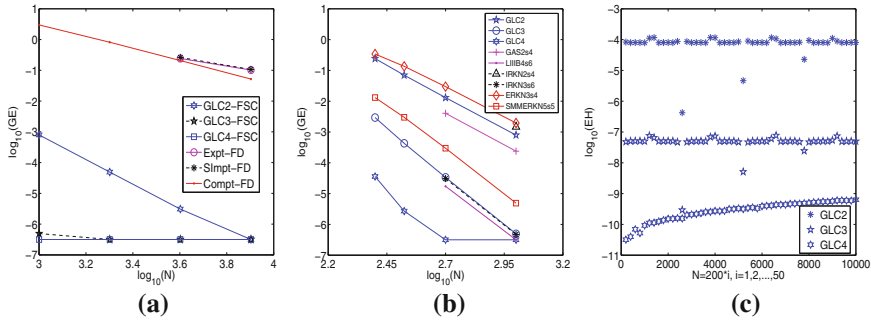


Fig. 11.3 The logarithms of the global error (GE) obtained by comparing our new schemes with the standard finite difference schemes (a) and the method-of-lines schemes (b) against different time integration stepsizes. c The conservation results of the GLCs with spatial discretisation by Fourier spectral collocation method ($M=400$). The time stepsize $\Delta t = 0.1$ for $T = 1000$

In Fig. 11.3a and b, the problem is integrated over the region $(x, t) \in [-20, 20] \times [0, 100]$ with different time stepsizes Δt and the spatial nodal values M . We compare our methods with the standard finite difference schemes in Fig. 11.3a. We choose $M = 1000$ for the finite difference schemes Expt-FD, SImpt-FD and Compt-FD and $M = 200$ for the time integrators GLCs coupled with the Fourier spectral collocation method (GLC-FSC). The logarithms of the global errors $GE = \|u(t_n) - u^n\|_\infty$ against different time stepsizes $\Delta t = 0.1/2^{j-1}$ for $j = 1, 2, 3, 4$ are displayed in Fig. 11.3a. In comparison with the method-of-lines schemes, we first discretise the spatial derivative by the Fourier spectral collocation method with fixed $M = 200$, and then integrate the semi-discrete system with different time stepsizes $\Delta t = 0.4, 0.3, 0.2$ and 0.1 . The efficiency curves are shown in Fig. 11.3b.

Besides, in Fig. 11.3c, the problem is discretised by the Fourier spectral collocation method with the fixed $M = 400$. We then integrate the semi-discrete system over the time interval $t \in [0, 1000]$ by the derived time integrators GLCs with the time stepsize $\Delta t = 0.1$. The numerical results in Fig. 11.3c present the error of the semi-discrete energy conservation law as a function of the time stepsize calculated by

Table 11.1 The total numbers of iterations for different error tolerances with $M = 400$ and $\Delta t = 0.1$ for $T = 100$.

	IRKN2s4	IRKN3s6	GAS2s4	LIIB4s6	GLC2	GLC3	GLC4
10^{-6}	2038	1996	4161	9309	1988	1988	1992
10^{-8}	2056	7967	7732	5745	2000	2000	2000
10^{-10}	2063	7579	8587	13519	2993	2993	2999
10^{-12}	2063	9508	45739	21820	3000	3000	3000

$\tilde{E}(t)$, where $\log_{10}(EH) = \log_{10}(|\tilde{E}(t_n) - \tilde{E}(t_0)|)$. We also display the total numbers of iterations in Table 11.1 when applying the different methods with different error tolerances to this problem for showing the efficiency of the fixed-point iteration in actual computations.

In conclusion, the numerical results demonstrate that the time-stepping integrators derived in this chapter have much better accuracy and energy conservation. They are more practical and efficient than existing methods in the literature.

Problem 11.2 We consider the nonlinear Klein–Gordon equation

$$\frac{\partial^2 u}{\partial t^2}(x, t) - a^2 \frac{\partial^2 u}{\partial x^2}(x, t) + au(x, t) - bu^3(x, t) = 0, \tag{11.136}$$

on the region $(x, t) \in [-20, 20] \times [0, T]$, subject to the initial conditions

$$u(x, 0) = \sqrt{\frac{2a}{b}} \operatorname{sech}(\lambda x), \quad u_t(x, 0) = c\lambda \sqrt{\frac{2a}{b}} \operatorname{sech}(\lambda x) \tanh(\lambda x),$$

with $\lambda = \sqrt{\frac{a}{a^2 - c^2}}$ and $a, b, a^2 - c^2 > 0$. The exact solution of Problem 11.2 is given by

$$u(x, t) = \sqrt{\frac{2a}{b}} \operatorname{sech}(\lambda(x - ct)). \tag{11.137}$$

The real parameter $\sqrt{2a/b}$ represents the amplitude of a soliton which travels with the velocity c . The potential function is $V(u) = \frac{a}{2}u^2 - \frac{b}{4}u^4$. The problem can be found in [39]. We consider the parameters $a = 0.3, b = 1$ and $c = 0.25$ which are similar to those in [39].

The Klein–Gordon equation 11.2 is solved by using the time integrator GLC4 coupled with the eighth-order symmetric finite difference method and the Fourier spectral collocation method. The graphs of errors are shown in Figs. 11.4 and 11.5 with the fixed time stepsize $\Delta t = 0.01$ and several values of M . The numerical results in Figs. 11.4 and 11.5 indicate that the Fourier spectral collocation method as a spatial discretisation method is much more accurate than the eighth-order finite difference method.

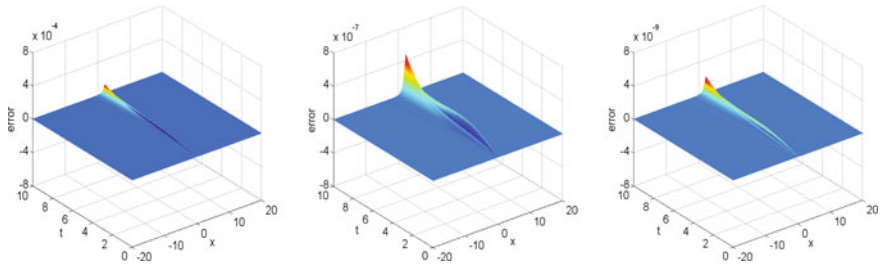


Fig. 11.4 The graphs of errors for the Klein-Gordon equation obtained by combining the time integrator GLC4 with the eighth-order finite difference spatial discretisation for the time stepsize $\Delta t = 0.01$ and several values of $M = 500$ (left), 1000 (middle) and 2000 (right)

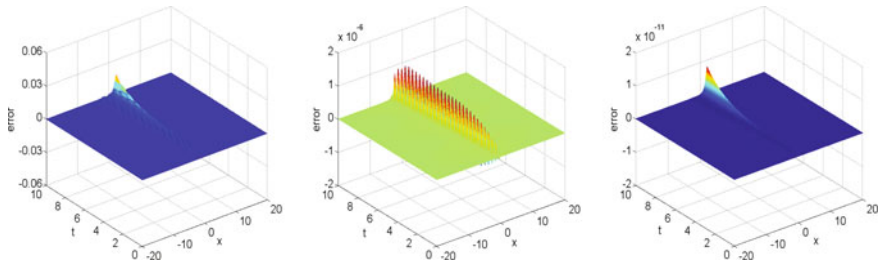


Fig. 11.5 The errors produced by combining the time integrator GLC4 with spatial discretisation by the Fourier spectral collocation method for the Klein-Gordon equation with the time stepsize $\Delta t = 0.01$ and $M = 200$ (left), 400 (middle) and 800 (right)

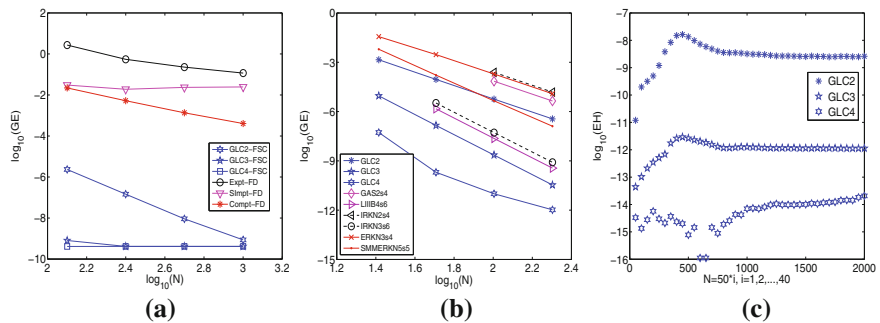


Fig. 11.6 The logarithms of the global error (GE) obtained by comparing our new schemes with **a** standard finite difference schemes and **b** the method-of-lines schemes against different time integration stepsizes. **c** The energy conservation results for the GLCs with spatial discretisation by the Fourier spectral collocation method ($M=200$). The time stepsize $\Delta t = 0.05$ for $T = 100$

In order to compare our methods with the classical finite difference schemes and the method-of-lines methods, we integrate the problem over the region $[-20, 20] \times [0, 10]$ with different time stepsizes Δt and spatial nodal values M . In Fig. 11.6a, we compare our methods with the classical finite difference schemes against different

Table 11.2 The total numbers of iterations for different error tolerances with $M = 800$ and $\Delta t = 0.1$ for $T = 100$

Tolerance	IRKN2s4	IRKN3s6	GAS2s4	LIIB4s6	GLC2	GLC3	GLC4
10^{-6}	2396	2000	5207	5566	686	686	975
10^{-8}	3871	3000	8585	7551	707	707	994
10^{-10}	6460	4568	12600	10659	1038	1038	1464
10^{-12}	9462	6139	16327	13800	1085	1085	1491

time stepsizes $\Delta t = 0.08/2^{j-1}$ for $j = 1, 2, 3, 4$. We use $M = 1000$ for the finite difference schemes Expt-FD, SI_{mp}t-FD and Compt-FD and $M = 600$ for the time integrators GLCs coupled with the Fourier spectral collocation method. We plot the logarithms of the global error in Fig. 11.6a. We discretise the spatial variable of the problem by the Fourier spectral collocation method with fixed $M = 800$ and integrate the semi-discretised system with the different time stepsizes $\Delta t = 0.4/2^{j-1}$ for $j = 1, 2, 3, 4$. The efficiency curves are depicted in Fig. 11.6b. The errors of the semi-discrete energy conservation law as a function of the time-step calculated by $\tilde{E}(t)$ are presented in Fig. 11.6c. Furthermore, the total numbers of iterations for different error tolerances are listed in Table 11.2.

It can be seen that the numerical results again indicate that our time-stepping integrators have higher precision than existing methods in the literature, and the qualitative property of energy preservation is also quite promising.

11.7.2 Simulation of 2D Sine–Gordon Equation

In this subsection, our time integration method **GLC4** coupled with *Discrete Fast Cosine / Sine Transformation* is used to simulate the two-dimensional sine–Gordon equation:

$$u_{tt} - (u_{xx} + u_{yy}) = -\sin(u), \quad t > 0, \quad (11.138)$$

in the spatial region $\Omega = (-a, a) \times (-b, b)$. The problem is equipped with the following homogeneous Dirichlet or Neumann boundary conditions, namely,

- *Dirichlet boundary conditions:*

$$u(\pm a, y, t) = u(x, \pm b, t) = 0; \quad (11.139)$$

- *Neumann boundary conditions:*

$$u_x(\pm a, y, t) = u_y(x, \pm b, t) = 0. \quad (11.140)$$

The initial conditions are

$$u(x, y, 0) = f(x, y), \quad u_t(x, y, 0) = g(x, y). \tag{11.141}$$

It is known that different initial conditions lead to different numerical phenomena. In what follows, we will use our method to simulate three different types of circular ring solitons. The initial conditions and parameters are chosen similarly to those in [12, 45].

Problem 11.3 For the particular case of circular ring solitons (see, e.g. [12, 45]), we select the following initial conditions:

$$f(x, y) = 4 \arctan \left(\exp \left(3 - \sqrt{x^2 + y^2} \right) \right), \quad g(x, y) = 0, \tag{11.142}$$

over the two-dimensional domain $(x, y) \in [-14, 14] \times [-14, 14]$. The simulation results and the corresponding contour plots at the times $t = 0, 4, 8, 11.5, 13$ and 15 are presented in Figs. 11.7 and 11.8 in terms of $\sin(u/2)$ for the mesh region size 400×400 and time stepsize $\Delta t = 0.1$. It can be clearly observed from Fig. 11.7 that the ring soliton shrinks at the initial stage ($t = 0$), but oscillations and radiations begin to form and continue until time $t = 8$. Moreover, it can be seen from the graphs that a ring soliton is nearly formed again at time $t = 11.5$. In Fig. 11.8, the contour maps depict the movement of the soliton very clearly. The CPU time required to reach $t = 15$ is 668.056765 seconds.

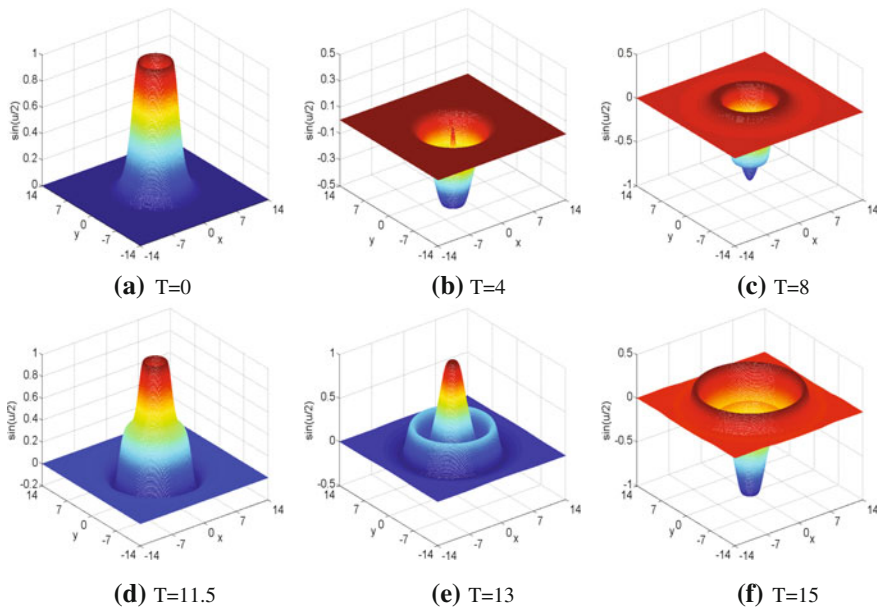


Fig. 11.7 Circular ring solitons: the function of $\sin(u/2)$ for the initial condition and numerical solutions at the times $t = 0, 4, 8, 11.5, 13$ and 15 , successively

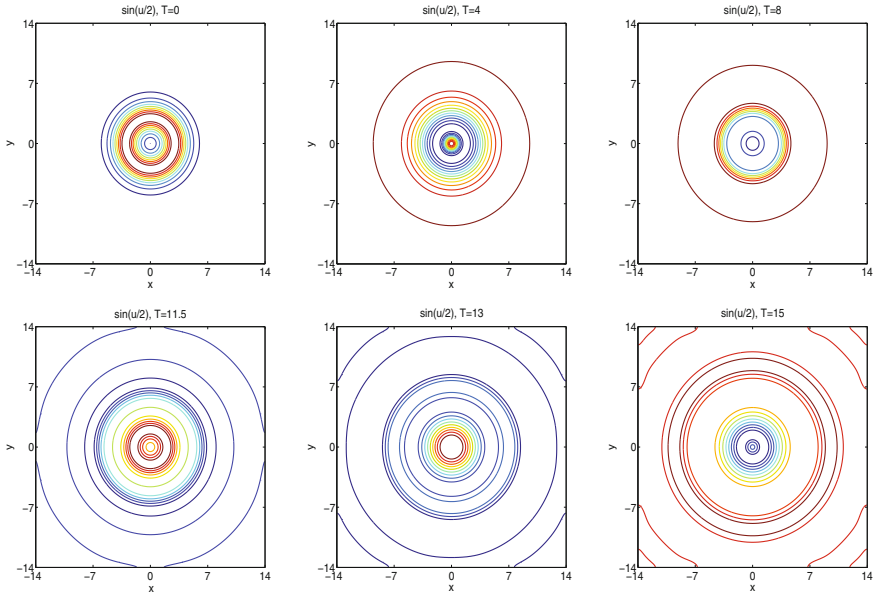


Fig. 11.8 Circular ring solitons: contours of $\sin(u/2)$ for the initial condition and numerical solutions at the times $t = 0, 4, 8, 11.5, 13$ and 15 , successively

Problem 11.4 Furthermore, if we choose the following standard setting:

$$\begin{aligned}
 f(x, y) &= 4 \arctan \left(\exp \left(\frac{4 - \sqrt{(x+3)^2 + (y+7)^2}}{0.436} \right) \right), \quad -10 \leq x \leq 10, \quad -7 \leq y \leq 7, \\
 g(x, y) &= 4.13 \operatorname{sech} \left(\exp \left(\frac{4 - \sqrt{(x+3)^2 + (y+7)^2}}{0.436} \right) \right), \quad -10 \leq x \leq 10, \quad -7 \leq y \leq 7,
 \end{aligned}
 \tag{11.143}$$

and extend the solution across the sides $x = -10$ and $y = -7$ using the symmetry properties of the problem, the phenomenon of the collision for two circular soliton will be occurred (see, e.g. [12, 45]). We compute solutions over the domain $(x, y) \in [-30, 10] \times [-21, 7]$ with the mesh region 800×400 and time step $\Delta t = 0.1$. The simulating results, as the function of $\sin(u/2)$, are depicted in Fig. 11.9 and Fig. 11.10. The numerical results in Fig. 11.9 demonstrate the collision between two expanding circular ring solitons, in which two smaller oval ring solitons bounding an annular region emerge into a larger oval ring soliton. The contour maps given in Fig. 11.10 show the movement of solitons much clearly. The CPU time required to reach $t = 10$ is 953.263314 s.

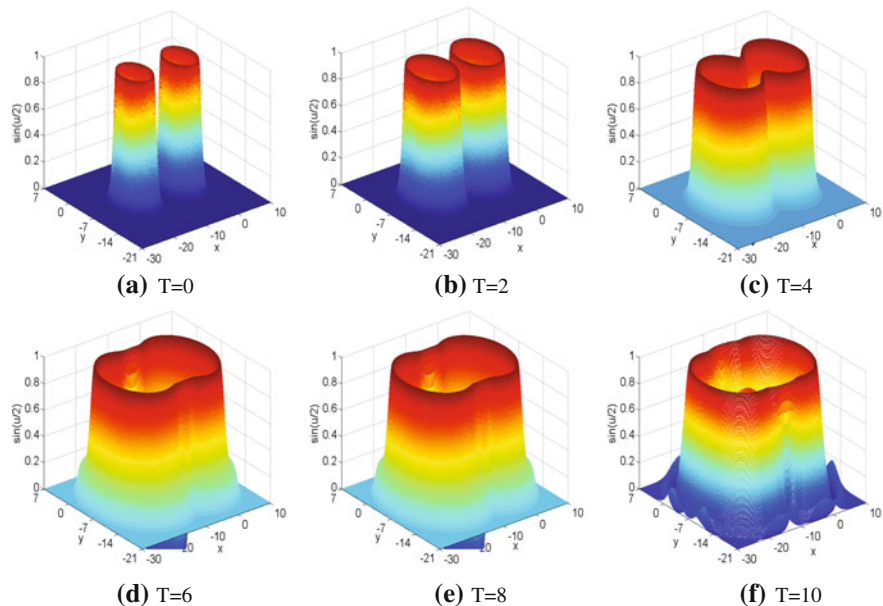


Fig. 11.9 Collision of two ring solitons: the function of $\sin(u/2)$ for the initial condition and numerical solutions at the times $t = 0, 2, 4, 6, 8,$ and $10,$ successively

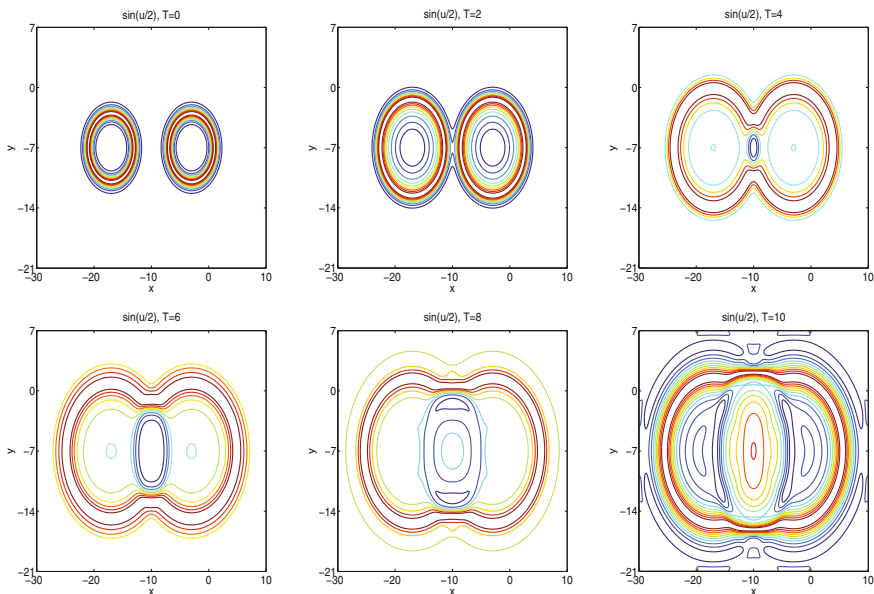


Fig. 11.10 Collision of two ring solitons: contours of $\sin(u/2)$ for the initial condition and numerical solutions at the times $t = 0, 2, 4, 6, 8,$ and $10,$ successively

Problem 11.5 Finally, for collisions of four circular solitons, we take

$$f(x, y) = 4 \arctan \left(\exp \left(\frac{4 - \sqrt{(x+3)^2 + (y+3)^2}}{0.436} \right) \right), \quad -10 \leq x, y \leq 10,$$

$$g(x, y) = \frac{4.13}{\cosh \left(\exp \left((4 - \sqrt{(x+3)^2 + (y+3)^2}) / 0.436 \right) \right)}, \quad -10 \leq x, y \leq 10. \quad (11.144)$$

The simulation of the problem over the region $[-30, 10] \times [-30, 10]$ is based on an extension across $x = -10$ and $y = -10$ due to the symmetry of the problem (see, e.g. [12, 45]). The size of mesh region used is 800×800 in space with the time stepsize $\Delta t = 0.1$. The numerical results are presented in Figs. 11.11 and 11.12 in terms of $\sin(u/2)$ at the times $t = 0, 2.5, 5, 7.5, 9$ and 10. Similarly to the case of the collisions for two circular solitons, the collision between four expanding circular ring solitons are precisely demonstrated in Fig. 11.11. The smaller ring solitons bounding an annular region emerge into a large one. Again, the contour maps plotted in Fig. 11.12 clearly show the movement of solitons. The CPU time required to reach $t = 10$ is 2492.677810 s.

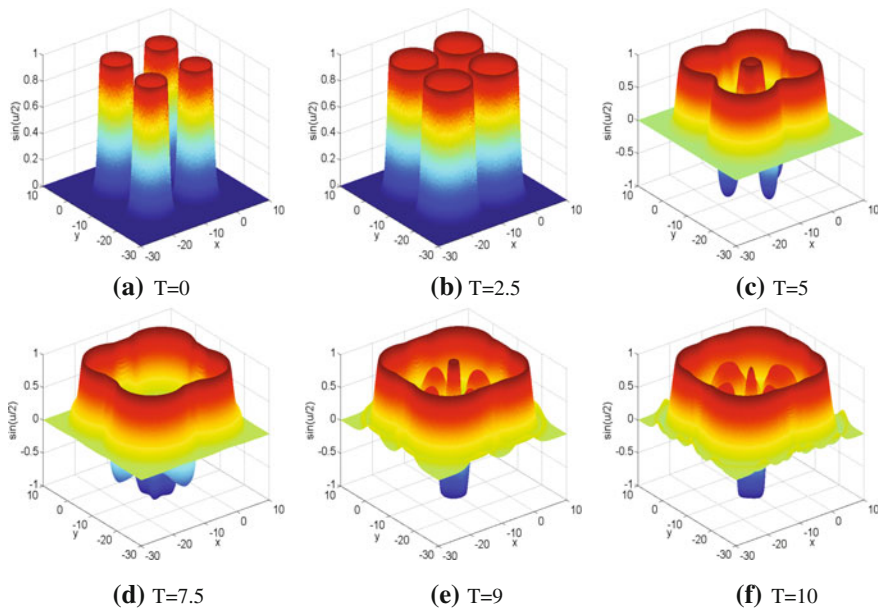


Fig. 11.11 Collision of four ring solitons: the function of $\sin(u/2)$ for the initial condition and numerical solutions at the times $t = 0, 2.5, 5, 7.5, 9$, and 10, successively

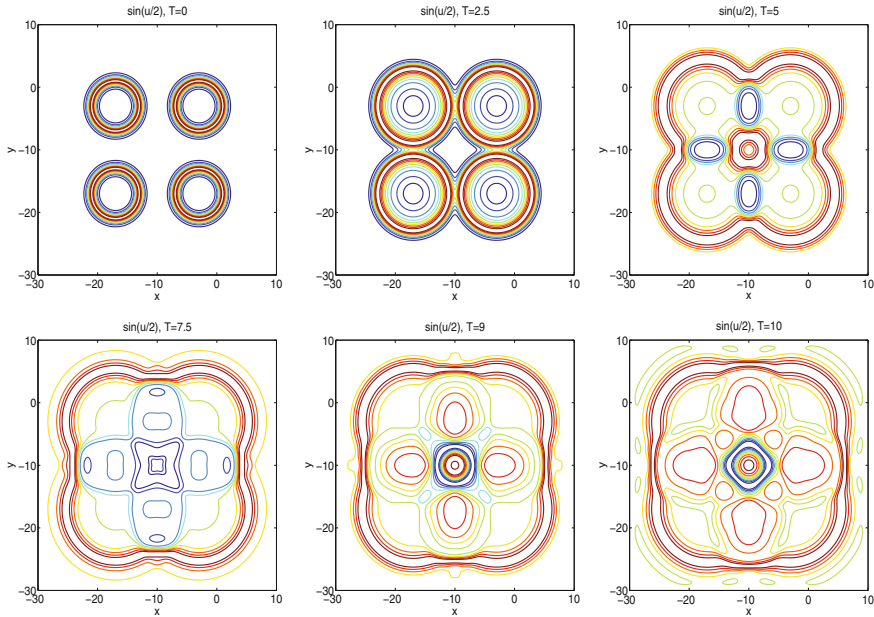


Fig. 11.12 Collision of four ring solitons: contours of $\sin(u/2)$ for the initial condition and numerical solutions at the times $t = 0, 2.5, 5, 7.5, 9,$ and $10,$ successively

11.8 Conclusions and Discussions

In this chapter, the nonlinear Klein–Gordon equation (11.1)–(11.2) was firstly introduced as an abstract ODE on the Hilbert space $L^2(\Omega)$ on the basis of the operator spectral theory. Then, the operator-variation-of-constants formula (11.14) was derived based on the well-known *Duhamel Principle*, which is in fact an integral equation of the solution for the nonlinear Klein–Gordon equation. Using the formula (11.14) and keeping the eventual discretisation in mind, a novel class of time-stepping methods (11.39) has been derived and analysed. It has been shown that under the simplified order conditions (11.48) and chosen suitable collocation nodes the derived time-stepping integrator can have arbitrarily high-order. The spatial discretisation is implemented, following a Lagrange collocation-type time-stepping integrator. This allows us to consider a suitable spatial approximation and gives us a great degree of flexibility when handling nonlinear potentials. The stability and convergence for the fully discrete scheme were rigorously proved after spatial discretisation. Since the fully discrete scheme is implicit and iteration is required, we used the fixed-point iteration (11.110)–(11.111) in practical computation and analysed the convergence of the iteration. Moreover, we also showed that our time-stepping integrators coupled with *discrete Fast Sine / Cosine Transformation* can efficiently simulate the important two-dimensional Klein–Gordon equations, equipped with Dirichlet

or Neumann boundary conditions. The numerical experiments carried out in this chapter clearly demonstrate that the time-stepping schemes have excellent numerical behaviour in comparison with existing methods in the literature. Last but not least, we again emphasize that all essential features of the methodology are present in the one-dimensional and two-dimensional cases in this chapter, although the schemes discussed equally lend themselves to higher-dimensional case. Moreover, remembering the eventual discretisation in space, applying a two-point Hermite interpolation to the nonlinear integrals that appear in the operator-variation-of-constants formula, we also can design different time schemes (see [40]).

The material of this chapter is based on the work by Liu and Wu [41].

References

1. Ablowitz, M.J., Kruskal, M.D., Ladik, J.F.: Solitary wave collisions. *SIAM J. Appl. Math.* **36**, 428–437 (1979)
2. Ablowitz, M.J., Herbst, B.M., Schober, C.: On the numerical solution of the sine-Gordon equation. *J. Comput. Phys.* **126**, 299–314 (1996)
3. Abramowitz, M., Stegun, I.: *Handbook of Mathematical Functions with Formulas, Graphs, and Mathematical Tables*. Dover publications, USA (1964)
4. Argyris, J., Haase, M., Heinrich, J.C.: Finite element approximation to two-dimensional sine-Gordon solitons. *Comput. Methods Appl. Mech. Eng.* **86**, 1–26 (1991)
5. Bank, R., Graham, R.L., Stoer, J., Varga, R., Yserentant, H.: *High Order Difference Method for Time Dependent PDE*. Springer, Berlin (2008)
6. Bártkai, A., Farkas, B., Csomós, P., Ostermann, A.: Operator semigroups for numerical analysis. In: *15th Internet Seminar* (2011–12)
7. Bařnov, D.D., Minchev, E.: Nonexistence of global solutions of the initial-boundary value problem for the nonlinear Klein–Gordon equation. *J. Math. Phys.* **36**, 756–762 (1995)
8. Bader, P., Iserles, A., Kropielnicka, K., Singh, P.: Effective approximation for the semiclassical Schrödinger equation. *Found. Comput. Math.* **14**, 689–720 (2014)
9. Bao, W.Z., Dong, X.C.: Analysis and comparison of numerical methods for the Klein-Gordon equation in the nonrelativistic limit regime. *Numer. Math.* **120**, 189–229 (2012)
10. Biswas, A.: Soliton perturbation theory for phi-four model and nonlinear Klein-Gordon equations. *Commun. Nonlinear Sci. Numer. Simul.* **14**, 3239–3249 (2009)
11. Bratsos, A.G.: A modified predictor-corrector scheme for the two-dimensional sine-Gordon equation. *Numer. Algorithms* **43**, 295–308 (2006)
12. Bratsos, A.G.: The solution of the two-dimensional sine-Gordon equation using the method of lines. *J. Comput. Appl. Math.* **206**, 251–277 (2007)
13. Brenner, P., van Wahl, W.: Global classical solutions of nonlinear wave equations. *Math. Z.* **176**, 87–121 (1981)
14. Briggs, W.L., Henson, V.E.: *The DFT: An Owners Manual for the discrete Fourier Transform*. SIAM, Philadelphia (2000)
15. Britanak, V., Yip, P.C., Rao, K.R.: *Discrete Cosine and Sine transforms: General Properties. Fast Algorithms and Integer Approximations*. Academic Press, Dublin (2006). ISBN 978-0-12-373624-6
16. Bueno-Orovio, A., Kay, D., Burrage, K.: Fourier spectral methods for fractional-in-space reaction-diffusion equations. *BIT. Numer. Math.* **54**, 937–957 (2014)
17. Cohen, D., Hairer, E., Lubich, C.: Conservation of energy, momentum and actions in numerical discretizations of non-linear wave equations. *Numer. Math.* **110**, 113–143 (2008)

18. Cao, W., Guo, B.: Fourier collocation method for solving nonlinear Klein-Gordon equation. *J. Comput. Phys.* **108**, 296–305 (1993)
19. Caputo, J.G., Flytzanis, N., Gaididei, Y.: Split mode method for the elliptic 2D sine-Gordon equation: application to Josephson junction in overlap geometry. *Int. J. Mod. Phys. C* **9**, 301–323 (1998)
20. Dehghan, M., Ghesmati, A.: Application of the dual reciprocity boundary integral equation technique to solve the nonlinear Klein-Gordon equation. *Comput. Phys. Commun.* **181**, 1410–1418 (2010)
21. Dehghan, M., Shokri, A.: Numerical solution of the nonlinear Klein-Gordon equation using radial basis functions. *J. Comput. Appl. Math.* **230**, 400–410 (2009)
22. Dehghan, M., Mohammadi, V.: Two numerical meshless techniques based on radial basis functions (RBFs) and the method of generalized moving least squares (GMLS) for simulation of coupled Klein-Gordon-Schrodinger (KGS) equations. *Comput. Math. Appl.* **71**, 892–921 (2016)
23. Dodd, R.K., Eilbeck, I.C., Gibbon, J.D., Morris, H.C.: *Solitons and Nonlinear Wave Equations*. Academic, London (1982)
24. Drazin, P.J., Johnson, R.S.: *Solitons: An Introduction*. Cambridge University Press, Cambridge (1989)
25. Duncan, D.B.: Symplectic finite difference approximations of the nonlinear Klein-Gordon equation. *SIAM J. Numer. Anal.* **34**, 1742–1760 (1997)
26. Ginibre, J., Velo, G.: The global Cauchy problem for the nonlinear Klein-Gordon equation. *Math. Z.* **189**, 487–505 (1985)
27. Guo, B.Y., Li, X., Vázquez, L.: A Legendre spectral method for solving the nonlinear Klein-Gordon equation. *Comput. Appl. Math.* **15**, 19–36 (1996)
28. Hairer, E., Lubich, C., Wanner, G.: *Geometric Numerical Integration: Structure-Preserving Algorithms for Ordinary Differential Equations*, 2nd edn. Springer, Berlin (2006)
29. Hesthaven, J.S., Gottlieb, S., Gottlieb, D.: *Spectral methods for Time-Dependent problems*. Cambridge University Press, Cambridge Monographs on Applied and Computational Mathematics (2007)
30. Hochbruck, M., Ostermann, A.: Explicit exponential Runge-Kutta methods for semilinear parabolic problems. *SIAM J. Numer. Anal.* **43**, 1069–1090 (2005)
31. Hochbruck, M., Ostermann, A.: Exponential Runge-Kutta methods for parabolic problems. *Appl. Numer. Math.* **53**, 323–339 (2005)
32. Hochbruck, M., Ostermann, A.: Exponential integrators. *Acta Numer.* **19**, 209–286 (2010)
33. Iserles, A.: *A First Course in the Numerical Analysis of Differential Equations*, 2nd edn. Cambridge University Press, Cambridge (2008)
34. Janssen, J., Vandewalle, S.: On SOR waveform relaxation methods. *SIAM J. Numer. Anal.* **34**, 2456–2481 (1997)
35. Jiménez, S.: Derivation of the discrete conservation laws for a family of finite difference schemes. *Appl. Math. Comput.* **64**, 13–45 (1994)
36. Kosecki, R.: The unit condition and global existence for a class of nonlinear Klein-Gordon equations. *J. Differ. Equ.* **100**, 257–268 (1992)
37. Lakestani, M., Dehghan, M.: Collocation and finite difference-collocation methods for the solution of nonlinear Klein-Gordon equation. *Comput. Phys. Commun.* **181**, 1392–1401 (2010)
38. Li, S., Vu-Quoc, L.: Finite difference calculus invariant structure of a class of algorithms for the nonlinear Klein-Gordon equation. *SIAM J. Numer. Anal.* **32**, 1839–1875 (1995)
39. Liu, C., Shi, W., Wu, X.Y.: An efficient high-order explicit scheme for solving Hamiltonian nonlinear wave equations. *Appl. Math. Comput.* **246**, 696–710 (2014)
40. Liu, C., Iserles, A., Wu, X.Y.: Symmetric and arbitrarily high-order Birkhoff-Hermite time integrators and their long-time behavior for solving nonlinear Klein-Gordon equations. *J. Comput. Phys.* <https://doi.org/10.1016/j.jcp.2017.10.057>
41. Liu, C., Wu, X.Y.: Arbitrarily high-order time-stepping schemes based on the operator spectrum theory for high-dimensional nonlinear Klein-Gordon equations. *J. Comput. Phys.* **340**, 243–275 (2017)

42. Lubich, C., Ostermann, A.: Multigrid dynamic iteration for parabolic equations. *BIT* **27**, 216–234 (1987)
43. Mulholland, L.S., Huang, W.Z., Sloan, D.M.: Pseudospectral solution of near-singular problems using numerical coordinate transformations based on adaptivity. *SIAMJ. Sci. Comput.* **19**, 1261–1289 (1998)
44. Pascual, P.J., Jiménez, S.: Vázquez, L. Numerical Simulations of a Nonlinear Klein-Gordon Model. *Lecture Notes in Computational Physics (Granada, 1994)*, vol. 448, pp. 211–270. Springer, Berlin (1995)
45. Sheng, Q., Khaliq, A.Q.M., Voss, D.A.: Numerical simulation of two-dimensional sine-Gordon solitons via a split cosine scheme. *Math. Comput. Simul.* **68**, 355–373 (2005)
46. Shen, J., Tang, T., Wang, L.L.: *Spectral Methods: Algorithms, Analysis, Applications*. Springer, Berlin (2011)
47. Strauss, W.A., Vázquez, L.V.: Numerical solution of a nonlinear Klein–Gordon equation. *J. Comput. Phys.* **28**, 271–278 (1978)
48. Sun, Z.Z.: *Numerical Methods of Partial Differential Equations*. Science Press, Beijing (2012). (2nd version, in Chinese)
49. Teman, R.: *Applied Mathematical Sciences*. In: *Infinite-dimensional dynamical systems in mechanics and physics*. Springer, Berlin (2000)
50. Tourigny, Y.: Product approximation for nonlinear Klein-Gordon equations. *IMA J. Numer. Anal.* **9**, 449–462 (1990)
51. Tang, W.S., Ya, Y.J., Zhang, J.J.: High order symplectic integrators based on continuous-stage Runge–Kutta Nyström methods. [arXiv:1510.04395](https://arxiv.org/abs/1510.04395)
52. Vandewalle, S.: Parallel multigrid waveform relaxation for parabolic problems. In: Teubner Stuttgart, B.G. (ed.) *Teubner Scripts on Numerical Mathematics* (1993)
53. Wazwaz, A.M.: New travelling wave solutions to the Boussinesq and the Klein-Gordon equations. *Commun. Nonlinear Sci. Numer. Simul.* **13**, 889–901 (2008)
54. Wu, X.Y., You, X., Wang, B.: *Structure-Preserving Algorithms for Oscillatory Differential Equations*. Springer, Berlin (2013)
55. Wu, X.Y., Liu, K., Shi, W.: *Structure-Preserving Algorithms for Oscillatory Differential Equations II*. Springer, Heidelberg (2015)
56. Wu, X.Y., Liu, C., Mei, L.J.: A new framework for solving partial differential equations using semi-analytical explicit RK(N)-type integrators. *J. Comput. Appl. Math.* **301**, 74–90 (2016)